RockSat-C 2018 Final Report
New Jersey Space Grant at
Stevens Institute of Technology

Vibration Isolation: To create a system that can record and isolate vibrations occurring in a payload during launch for sensitive electronics. The system will be inexpensive and will consist of commodity hardware with a small footprint.

Pressure Sensor: To create a Data Acquisition Unit which can record data from a pressure sensor located on the skin of the rocket, with the interest of analyzing high-speed aerodynamic phenomena. In particular, boundary layer transitions are expected to occur when the rocket approaches high speeds, on the order of Mach 4.

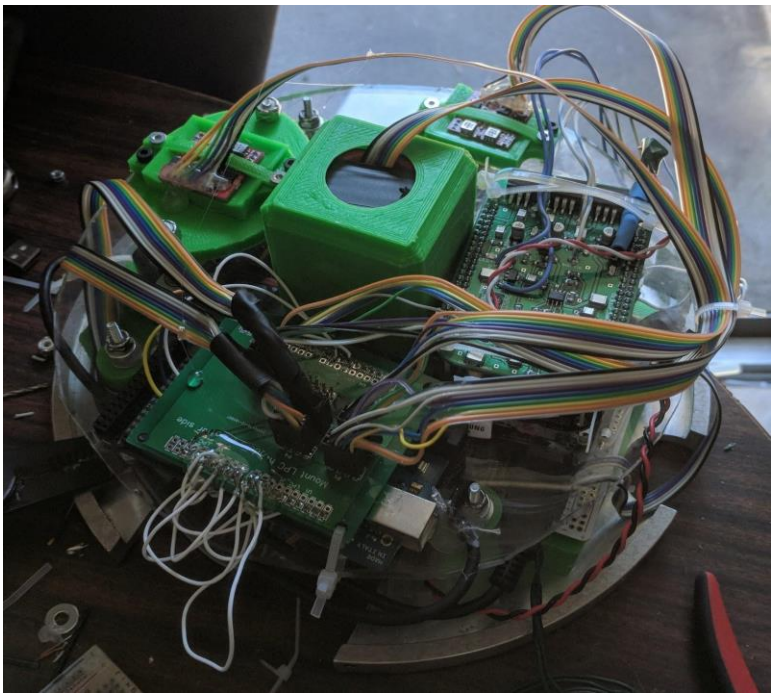

Vibration Isolation: Andrew Afflitto, Aidan Aquino, Joshua Gross, Stephen Kontrimas, Jesse Stevenson, Zachary Shoop, Adam Testa, Samuel Yakovlev
Pressure Sensor: Ronald Ankner, Alexandria Austin, Christopher Blackwood, Christopher Cowan, Richard Thornton
Advisors: Professor Joseph Miles and Professor Nick Parziale
School: Stevens Institute of Technology
Submittal Date: July 30th, 2018

Part 1: Vibration Isolation

1.0 Mission Statement:

The goal of this project was to create a system that can record and isolate vibrations. The payload will have a small footprint so as to fit comfortably in the canister. This experimental system would be used to house sensitive electronics like a mass spectrometer. The project will be produced with commodity hardware. The objectives laid out by this project were to have results comparable to last year's data and to have a reusable payload that could be used in future launches -- particularly, the reusability of the data acquisition system was of interest.

2.0 Mission Requirements and Description:

A rocket launch produces large amounts of vibrations during launch. For the purposes of this experiment, the targeted frequencies were from 200 Hz to 22 kHz, which happen to be the approximate range of human hearing. According to the Nyquist Theorem, the data acquisition system must sample at twice the highest frequency to ensure no information is lost, so the data acquisition must be sampled at 44 kHz to achieve the full 22 kHz bandwidth. The 2017 RockSat-C launch used single axis accelerometers, whereas the goal of this year's team was to use two axis accelerometers. This doubles the required bandwidth and data storage. Because the goal of the project was to observe vibrations during launch, the experiment started by booting the Beaglebone at T -3 and then immediately started data collection and continued to collect data until storage was full.

There were two types of systems designed for this project: passive and active. Due to time constraints, only the passive systems were implemented in the payload. The passive systems are simple, with a material chosen to act as a damper. Each accelerometer represents a small payload and the damping material is mounted to isolate vibrations from the accelerometer.

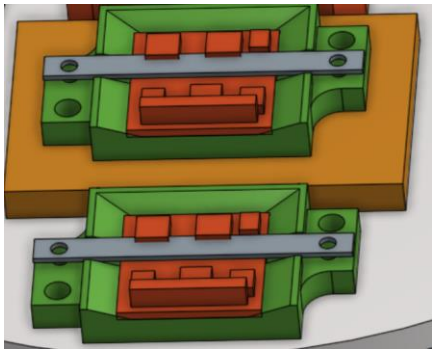

Figure 2.1: A comparison between mounting passive accelerometers. The bottom setup contains no damper and behaved as the control accelerometer

There is another different type of passive system included in the payload, the magnetic passive system or MaPS for short. This system functioned the same in principle as the material damper based ones. The differences between the two dampers is that the material damper is replaced by a magnetic damper.

The active system was more ambitious than last year's active system. Previously, a solenoid was used to induce a change in acceleration. Solenoids are binary in state, so last year's system wound up inducing more jerk. A goal of the active system this year was to allow for smoother actuation. A proof of concept using a spool of wire and a magnet to make a voice coil actuator was completed, but had to be abandoned because of time constraints.

3.0 Payload Design:

There were two main design endeavors for the payload, which consisted of the mechanical layout and the data acquisition board with its associated electrical requirements. The team dealt with the electrical system first, as its requirements drove the mechanical layout. The electrical system was broken down into the power supply, data storage, digital conversion, and the accelerometers themselves.

The electrical design required implementation of a custom accelerometer breakout board, Beaglebone Black, eight LiPo batteries, and a data acquisition board using an NXP LPCxpresso 43S67. The power supply was made up of the eight batteries, as well as a power distribution board used a Recom Power R-78E5.0-0.5 voltage regulator in order to supply a steady voltage to the system. The power distribution board is shared with the pressure sensor team's experiment and uses MOSFETs to switch the main power from the T-3 min activation line. The power board directly powers the 5V in of the Beaglebone which powers the LPC board over it's USB host connector.

Originally the intention was to use only the beaglebone for data acquisition, but this proved to be too difficult to achieve due to the nature of the board and overheads from the linux kernel. To accommodate, an additional microcontroller was added to reduce the overhead in reading results from each sensor. The LPCxpresso chip acted as the controller which read off the data from the sensors using a common SPI data line, sharing the MISO, MOSI, and trigger (CNVST) lines. The LPC microcontroller cycles through the chips, by having separate chip select GPIO pin for each of the accelerometer boards being read. This would in effect have only one of the accelerometers using the SPI line at a time, which meant that, if cycled through quickly enough, the required data could be obtained from all of the given accelerometers. During the integration and assembly of the payload for vibration testing, the LPC microcontroller was damaged causing a short in the main processor chip. As no spare LPC board was on hand the team had to replace the LPC board with an Arduino Mega on hand for the electronics that launched with the rocket.

The accelerometers breakout boards themselves were small, one inch by one inch, boards designed to deliver a two axis accelerometer readings to the SPI line. This was made up of two

one axis ADXL001 accelerometers, positioned orthogonally from one another, fed into a 4-channel MAX11618EEE ADC, of which only the first two channels were used. The analog accelerometer signal was also passed through a notch filter to reduce a resonance, which was recommended by the manufacturer.

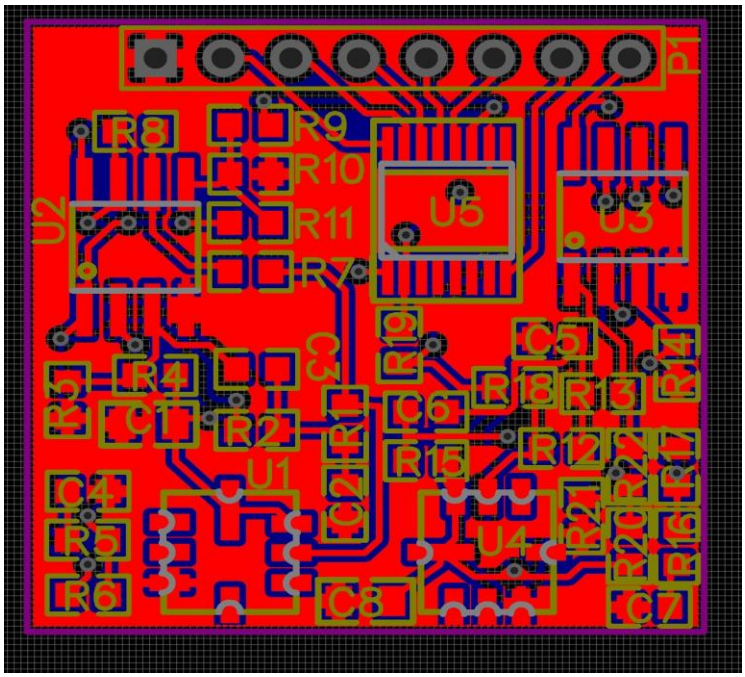

Figure 3.1: Accelerometer breakout board layout

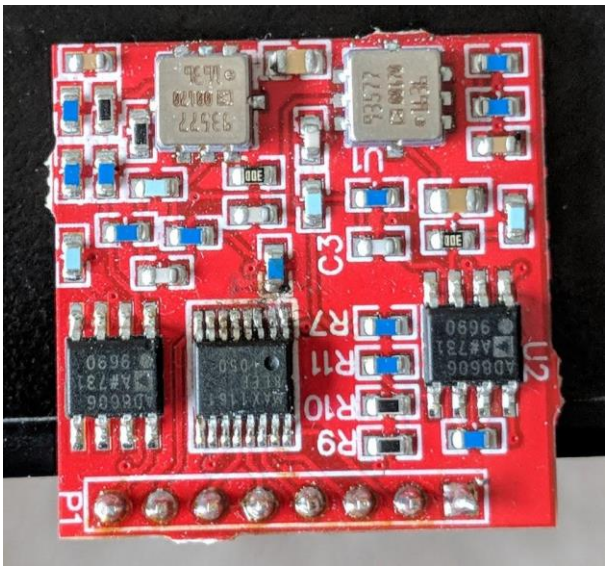

Figure 3.2: Physical accelerometer breakout board with perpendicular mounted accelerometers

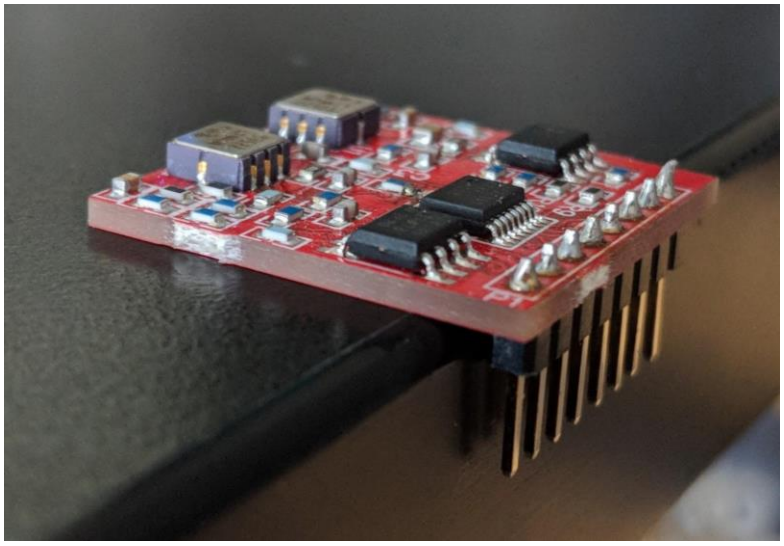

Figure 3.3: Side view of the accelerometer with pins showing the relative z-sizes of parts

The USB data line between the LPC chip and the Beaglebone Black transfers the combined data from all of the accelerometers using a Virtual COM interface.

Moving onto the mechanical design, the following parts needed mounting: the eight batteries, the LPCxpresso, Beaglebone Black, the three passive material accelerometers, one control, one magnetic passive system and any pressure sensor equipment.

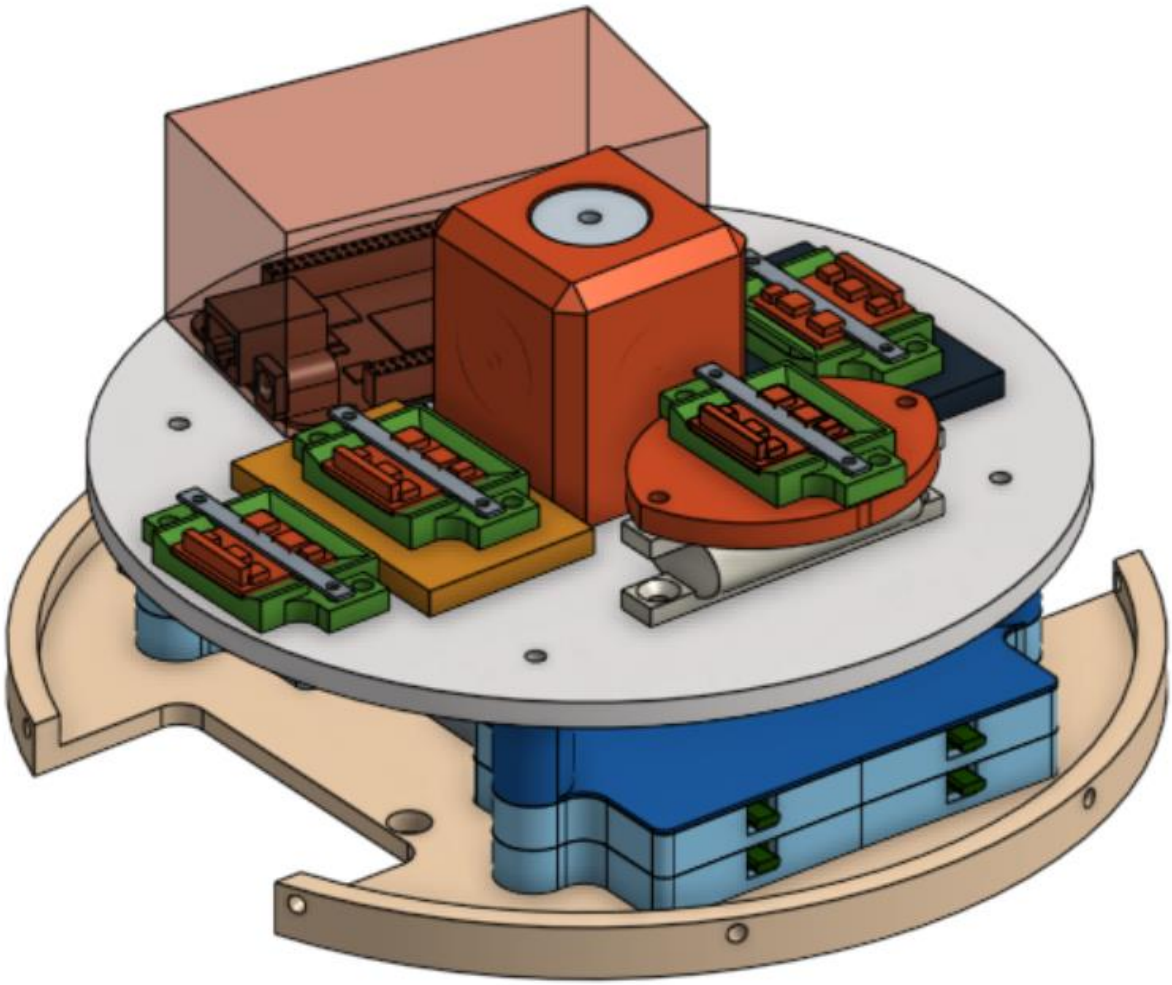

Figure 3.4: CAD model of the Canister

In Figure 3.4, all the passive damper accelerometers are mounted on a top plate along with the control, and the MaPS (large red box) are mounted on a raised circular plate. The Beaglebone Black, with a red clearance box placed around it, is for the Pressure Sensor team. Mounted using the same holes, obscured in Figure 3.4, is the Beaglebone Black for the Vibration Isolation team. On the bottom, mounted on the midplate and holding the circular plate up, are the eight lithium polymer batteries which provide all the power for the vibration isolation systems.

The passive vibration system consisted of three accelerometers, which were placed upon three different isolators. The first vibration isolator was a Sorbothane Polyether-Based Polyurethane pad. This material was used as an isolator in the 2017 launch, and managed to significantly reduce the vibrations experienced by the accelerometer. The Polyurethane pad was chosen again for this project to act as a reference for this year's project, as well as to see if it would perform similarly to last year's, which would allow the team to determine the comparability between the current project and last year's project. The second material used was a Neoprene black pad. Neoprene is a polymer that is commonly used in sound and vibration dampening, which made it a good choice for reducing the vibrations experienced by the

accelerometer. The final isolator, excluding the MaPS system, was a cable mount purchased from dB Engineering. Unlike the previous two isolators, the cable mount uses springs to reduce vibrations. The springs absorb extraneous vibrations, and dissipate them without allowing the accelerometer to experience much movement. Of the three passive vibration isolators, the cable mount was expected to perform the best in reducing and eliminating vibrations.

4.0 Student Involvement:

RockSAT at Stevens is organized as a volunteer project for those interested in rocketry rather than as part of a class or as research. As there are no credits involved it can be sometimes be de-prioritized over other obligations by some members resulting in some members contributing significantly more than others. The following members listed were the most active during the entire year.

Andrew Afflitto - designed the data acquisition system.
Aidan Aquino - selected the passive material.
Joshua Gross - designed the data acquisition system.
Stephen Kontrimas - designed the active system development was mechanical and project lead.
Jesse Stevenson - designed the data acquisition system and was the electrical lead.
Zachary Shoop - designed the data acquisition system.
Adam Testa - overhauled and made many revisions to the canister design.
Samuel Yakovlev - designed the passive magnetic passive system.

5.0 Testing Results:

Throughout the design process of the payload, incremental tests were done as different components were completed.

After the accelerometer breakout board design was completed, manufactured, and assembled, testing and integration started immediately. The breakout boards were tested initially using a frequency generator as the analog input of the accelerometer to verify that no samples were dropped or distorted. This was tested at a low-sampling rate using an Arduino to ensure the system was working. The team tested the accelerometer boards by using Arduino's Serial Plotter in order to examine the accelerometer data on a graphical interface. The results of a sine wave input processed by the A/D converter is shown in figure 5.1 below. The test setup is shown in figure 5.2.

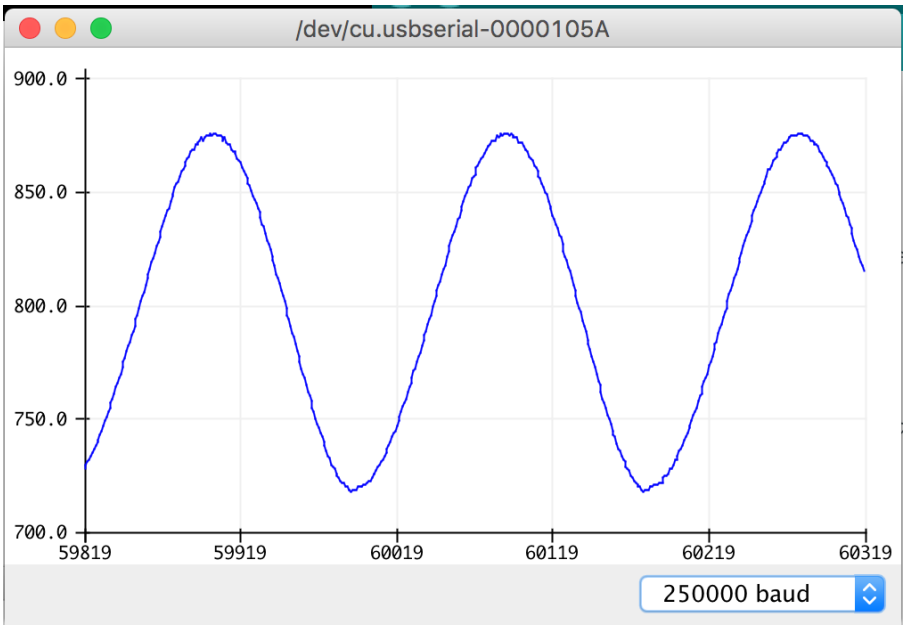

Figure 5.1: Arduino Serial Plotter Output of a Sinusoidal Input on the SPI A/D Converter

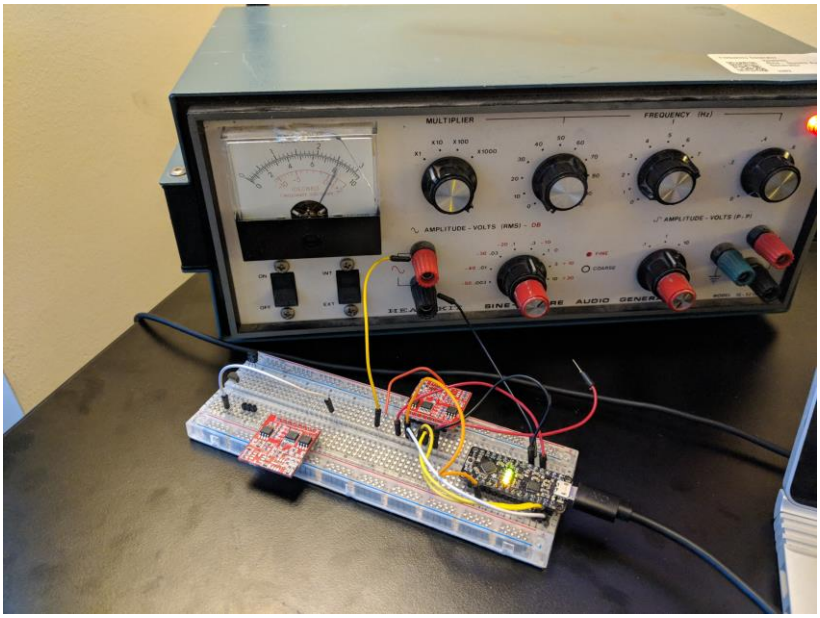

Figure 5.2: Test Setup Used to Perform the Sinusoidal Test

As this test went successfully, the accelerometers were then soldered on using a hot air soldering station with solder paste. The accelerometer connections were tested by moving the accelerometer aggressively. The graph would spike and peak for the duration of the movement indicating that the accelerometer is functioning. Testing was then performed on reading both the X and Y channels of each board simultaneously.

After a single accelerometer as determined to be working successfully, the test setup was upgraded to be able to read multiple accelerometers on the same SPI bus using GPIO pins as chip select lines while still using the Arduino. The same behavior was then observed as with two

accelerometer boards as it was with one, and the full suite of six was tested to be operable in the Arduino environment. This was also verified using a logic analyzer to confirm the signals were correct from each of the boards.

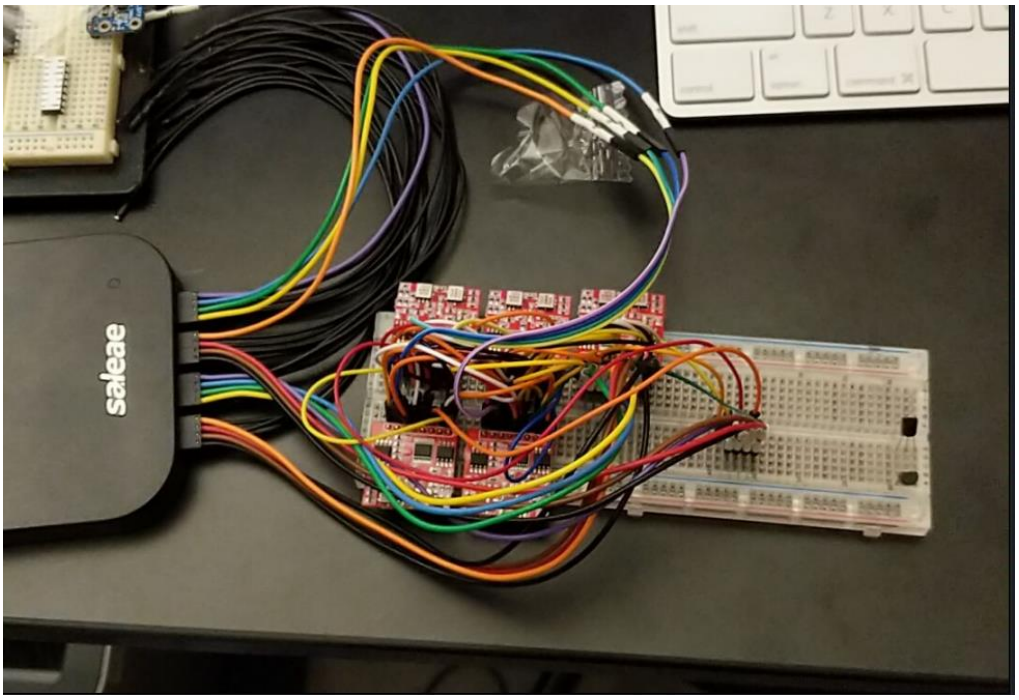

As the original intention was to use the Beaglebone's integrated SPI buses to communicate to all the accelerometers using either the Linux device files in the file system, modifying the switch matrix of the CPU in order to obtain the required SPI clock and read speeds, or staging the design by having the built in PRU (Programmable Realtime Unit) microprocessors obtain the data from the SPI buses and write using DMA to memory, which the CPU wrote into the file system, but under the current provided Linux kernel this proved to be quite a challenge. Various boot arguments and special changes to the kernel needed to be made in order to obtain a file system argument capable of sending SPI communications over it, and communicating using direct memory access was determined to be out of scope for a project of this caliber as there was little working documentation working for the beaglebone in this functionality. The team debated switching to an older kernel, but it was eventually determined that switching to the LPCXpresso chip would be more beneficial as the board fit more closely with our use case, as it had faster GPIO, and more specifically, SPI capabilities, and hardware USB2 support.

6.0 Mission Results:

Below in Figures 6.1 and 6.2 show the data recorded from data recorded from the launch. The spectrogram data does not match the footprint of vibration data, and is surprising.

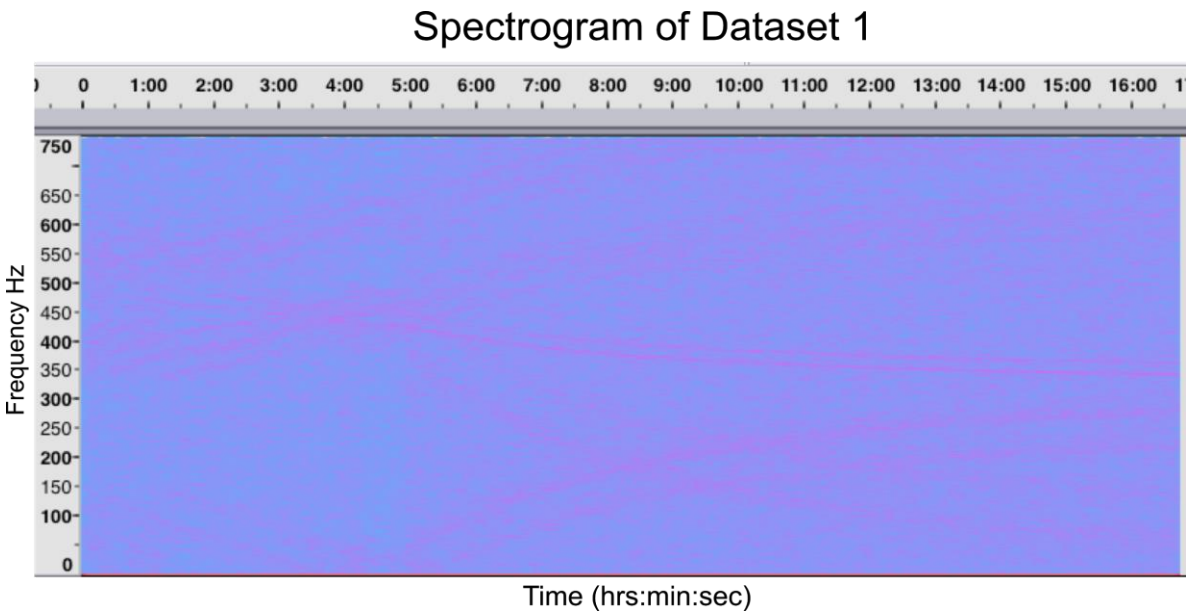

Figure 6.1: Audacity spectrogram of the X-accelerometer during launch

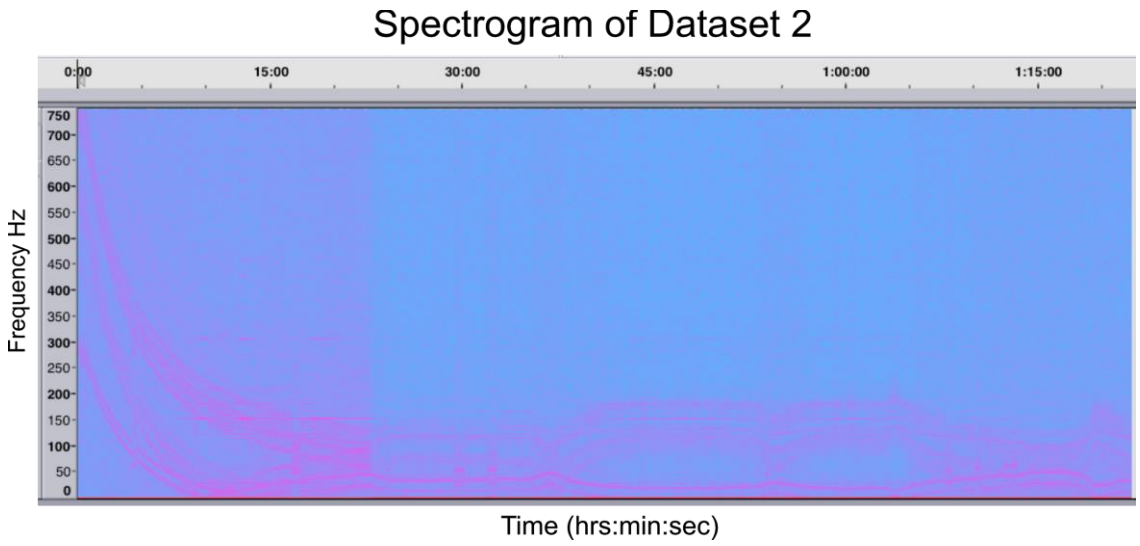

Figure 6.2: Audacity spectrogram of the X-accelerometer after splashdown

Interestingly the data recorded appears to be a strong correlation between temperature and time. The temperature can be seen below in Figure 6.3 from UA and ASU's payload.

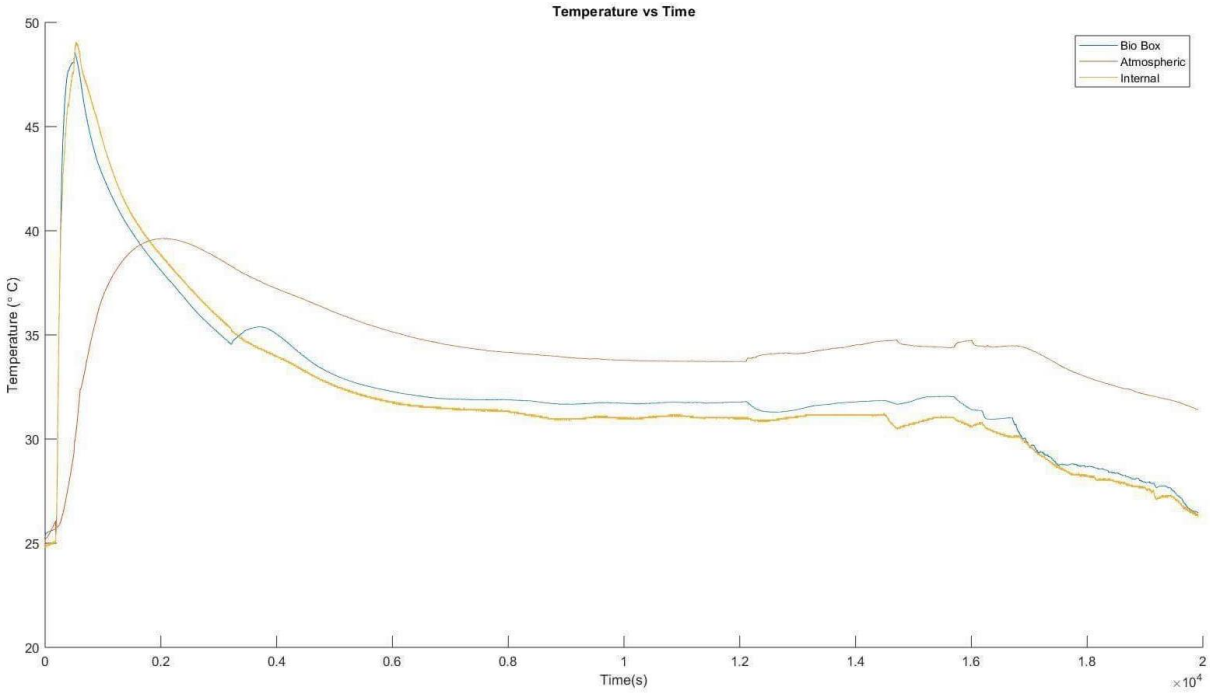

Figure 6.3: Temperature data provided by UA and ASU's payload for comparison (credits: Joel and Sean Hopta from the A.Z.S.G.C.)

Even though no data was retrieved from the flight itself, the team took the opportunity to investigate the cause of data failure, get the electronics fully operational, and perform a vibration test to fulfill some of the original objectives from the experiment.

The first priority was to determine the current state of the electronics after launch and determine if the problems experienced during launch were persistent. To minimize the number of random variables the system was tested with the data acquisition Arduino and accelerometers only, disregarding the power system and Beaglebone. Attaching the Arduino's USB directly to the computer revealed that the problem was persistent, showing only one accelerometer data on one channel. During integration several wires broke off to two of the accelerometer breakout boards that caused the failure. Due to a flaw in the design of the custom boards only discovered after launch, if any of the chip select wires was disconnected from the breakout boards, it will "talk over" the data from other accelerometers. This configuration of the SPI bus is known as having an active low chip select line. To fix this, a pull-up resistor should have been added in the breakout board schematics, which would prevent any A/D converters from communicating if the CS line was disconnected. This problem was observed by recording the analog waveform of the digital MISO line. As shown in Figure 5.1, the signal from the first accelerometer is measured at 2.321 V when sending a '1'. This is close to or below the usual threshold for binary values, which results in zeros being read on most channels. As the read cycle gets to the 5th chip, the signal returns to its nominal 5V value indicating that there were multiple drivers active on the MISO pin.

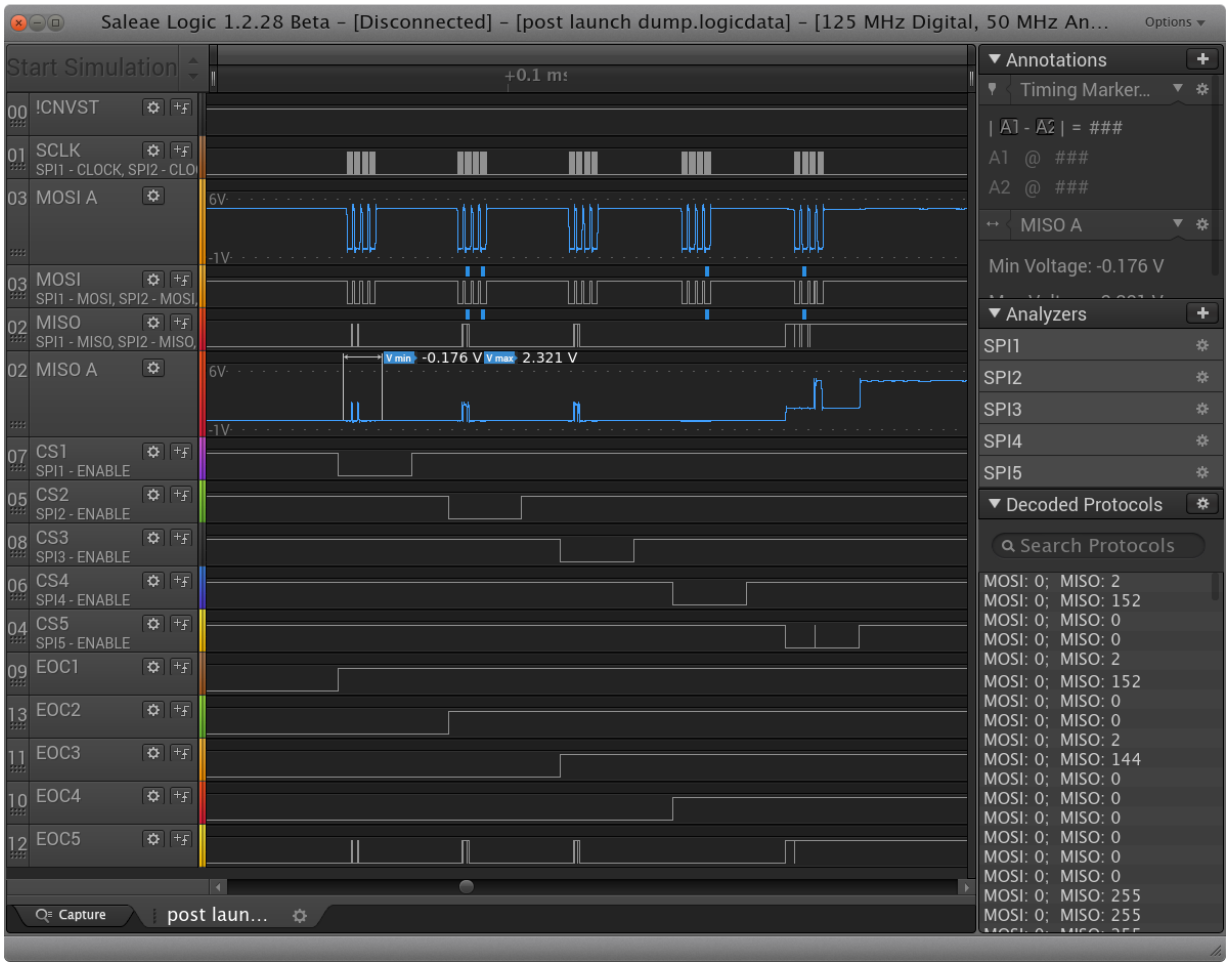

Figure 6.4: Arduino Electronics Waveform Showing Multiple Drivers

As the Arduino electronics were a last minute replacement for the payload electronics, it was decided that the team should continue any testing of the payload with the original design and a new (not fried) LPC board. The objective of this test was to get the electronics fully working, report on any flaws found and fixed, and to perform a vibration test using a homemade vibration table to demonstrate feasibility of the system. The software for the LPC board was a bit behind so the first step was to update the setup routines for the accelerometers to ensure they had the correct configuration to read both channels reliability. This step is documented in the Github commits done to the LPC_SPI repository listed in the appendix section of this document.

The accelerometers were found to be very sensitive to disconnects on the crimped connections. A lot of time was also put into tuning the timing of the sample triggers and when the samples were read to ensure that all accelerometers were able to respond with correct data. A sampling rate of 12.5 kHz sampling rate was achievable with the current configuration. The main limiting factors for the team being able to achieve the full 22 kHz sampling rate is the time it takes to transfer the data from each accelerometer serially. If the team wanted to improve on this sampling rate, the team could use the other two cores on the NXP LPC microcontroller to run two or more SPI transactions at once to reduce this delay. The next bottleneck found was with

the virtual com port implementation. As a vcom interface emulates a serial port, there is a lot of overhead traffic that can saturate a regular USB 2.0 interface with the data rates being sampling at. This might be solved using larger "packet" sizes by sending more than one sample data per transaction, or switching to using a lower level USB protocol such as libusb. Depending on the computer and how busy the USB bus is the team was seeing a loss of 512 samples when trying a sampling rate of 17 kHz. For the validity of the post-launch vibration experiment, the team lowered the sampling rate to 12 kHz to fix the dropped samples problem for now.

One of the accelerometer breakout boards had a disconnected pin on one of the A/D converters. During original testing the team tried unsuccessfully to solder a small wire to the SMD pads of the A/D converter to test the board without any filter circuitry. The damaged pin was re-soldered, but apparently had disconnected during launch. This may explain the noise on the one working channel during launch. When pushing on this pin, the pin reconnects and the A/D converter reads the values correctly. As the pads on the A/D converter are too small to hand solder without the proper tools, it is much easier in this case to use replacement boards instead of trying to repair small leads. The team had ordered another spare set of 6 boards but the they were not delivered until after the launch as they were delayed.

The team does not have access to a vibration table for testing the experiment on, to test the accelerometers to ensure they are sampling correctly, a Dewalt orbital sander was mounted to a piece of wood using some canvas, staples, and glue. This was speed controlled using a variac. The input voltage correlates well to the frequency of vibration, allowing the team to test a range of frequencies from 0 Hz to 300 Hz. This is on the low end of the target range of the project, but will still confirm that the accelerometers are working. Pictures of this setup are shown in figure 6.5 and 6.6 below.

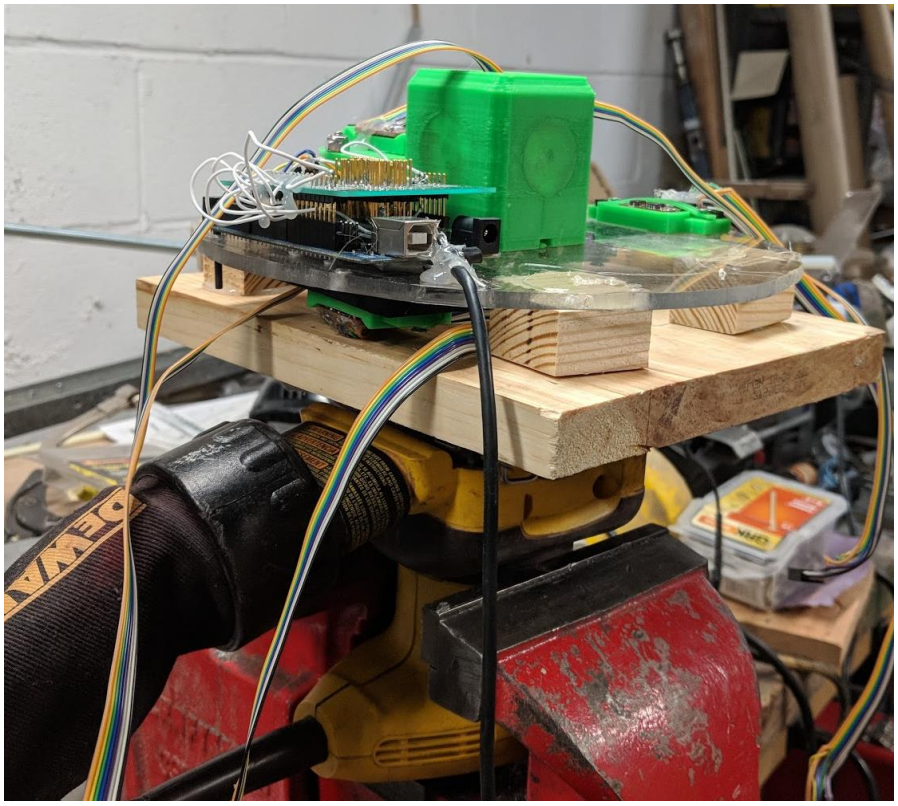

Figure 6.5 - Orbital Sander vibration testing

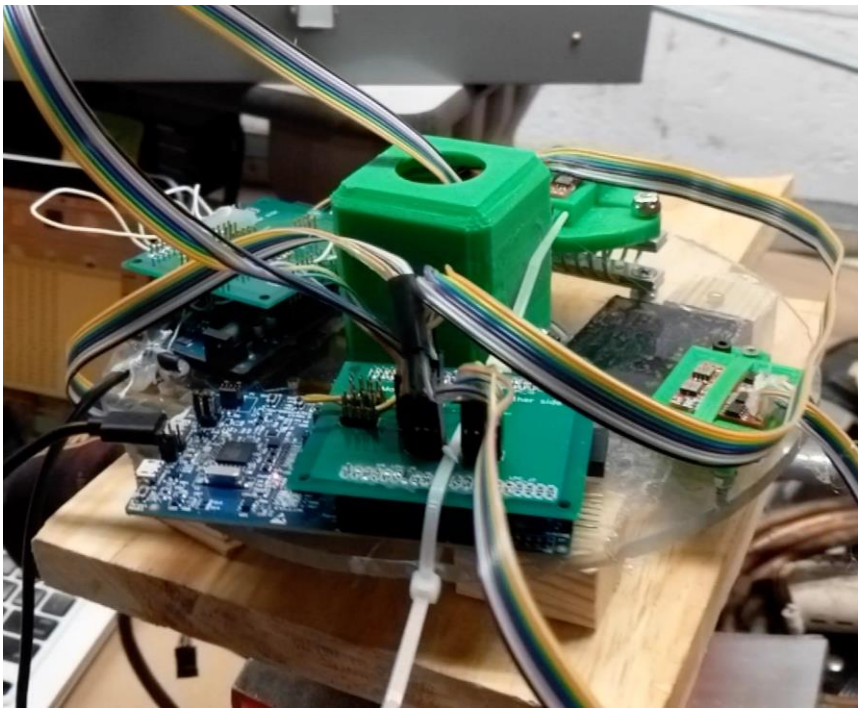

Figure 6.6 - Test Setup with original NXP LPC43S67 Board

Figure 6.7 Sander Attachment to the Testing Platform

The results from the post launch analysis are shown on the following pages. The DC offset of the data was removed by subtracting the mean of the data in MATLAB. Figure 6.8 is an amplitude vs time graph of the data labeled for each channel.

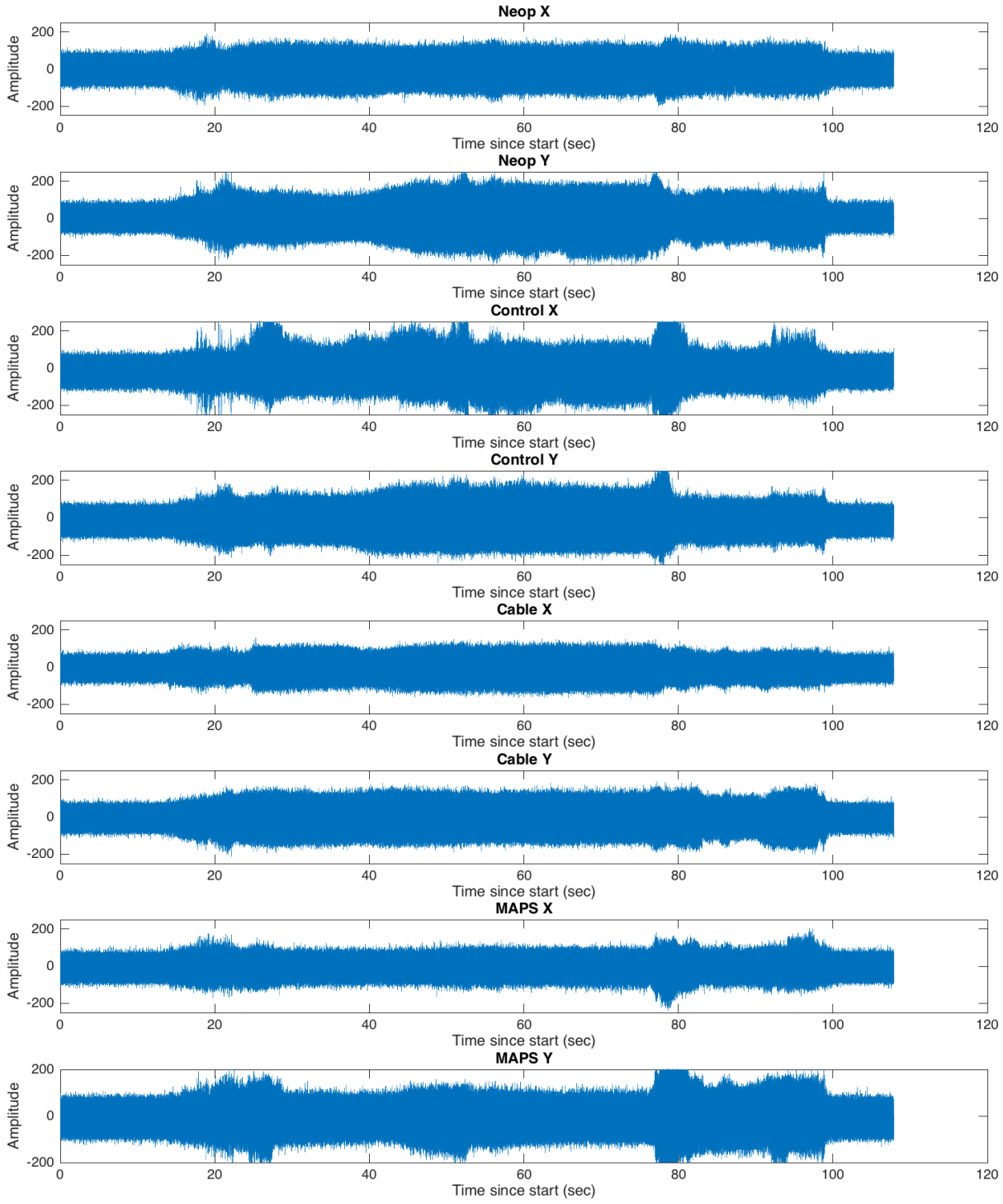

Figure 6.8: Amplitude vs Time Graph of Post-launch Test Data

Figure 6.9 is a spectrogram showing a graph of frequency vs time. The amplitude of each frequency component is represented using a color scale.

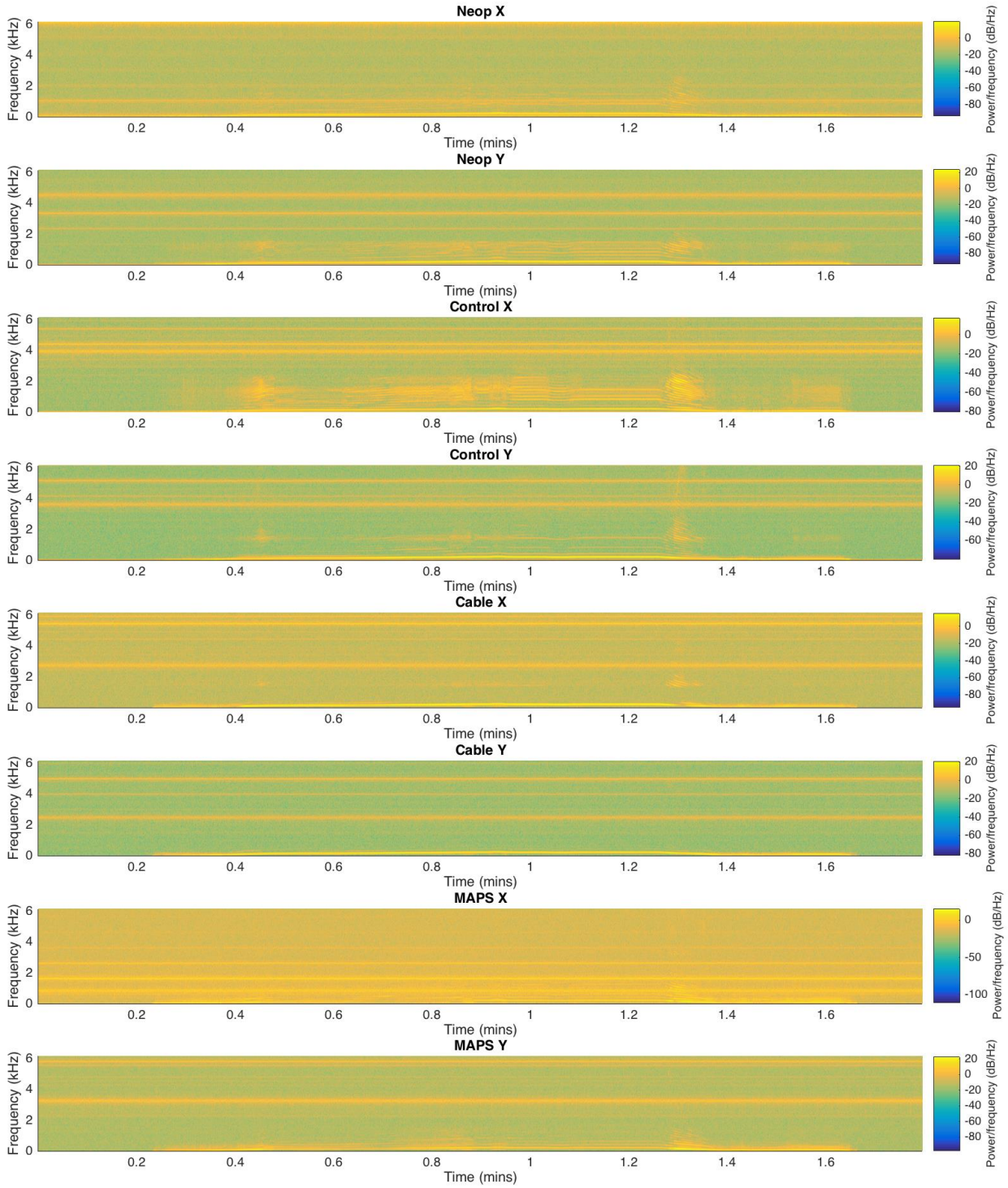

Figure 6.9: Spectrogram of Post-launch Test Data

Figure 6.10 shows the relative power

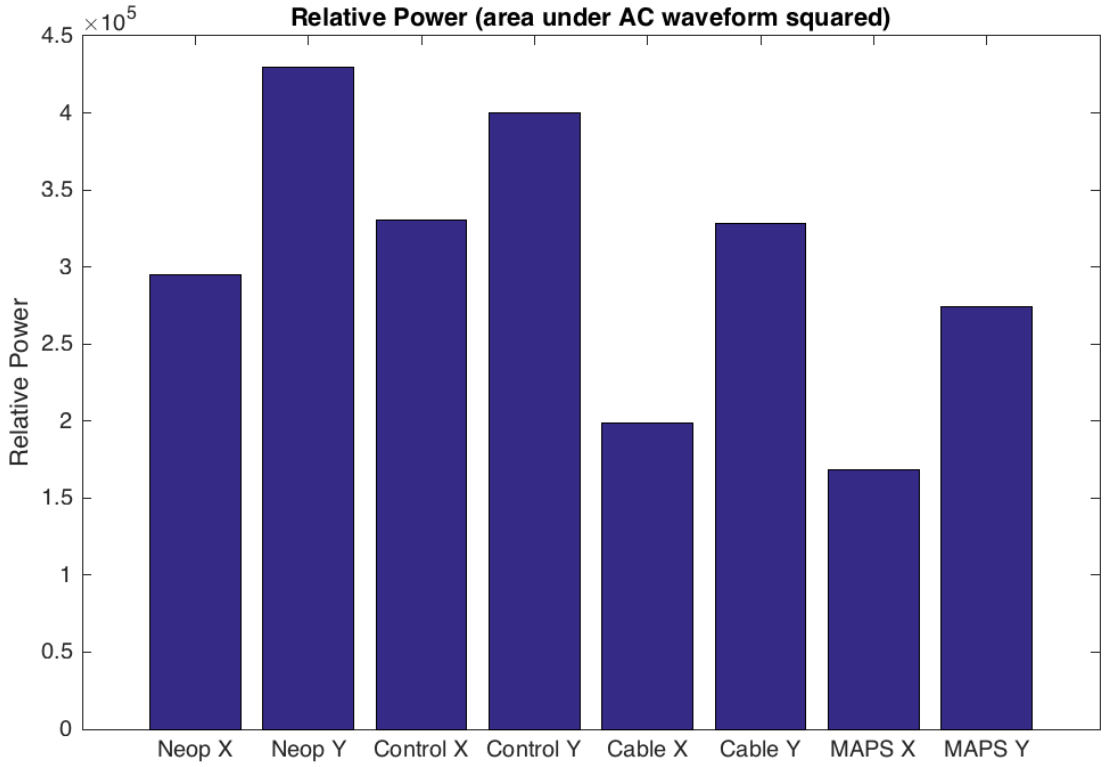

Figure 6.10: Relative Power of Post-launch Test Data

During testing the team realized that glue used as a wire strain relief in this test setup touched the surface of the vibration table due to the standoffs not being long enough. This caused the foam neoprene sample to have the highest amount of vibration out of all of the samples. The other sample specimens appear to have sensible data all showing decreases in power from the control. The difference in the X and Y channels of all of the samples is likely due to how the payload was attached to the orbital sander. As the samples were attached using a loop of canvas stapled to the bottom of a wooden board, vibrations may not be transferred well in the direction orthogonal to the loop axis. Explained simply, the loop lets the sander slide a small distance in the X axis. This attachment is shown in figure 6.7. This could be improved by either providing a method of tightening the canvas piece after mounting to remove the slop or by using a more rigid attachment to the sander output. One approach could be to lengthen the bolts located under the sanding pad to have a direct attachment.

The cable mount shows interesting results as it shows better isolation performance in the X axis than the Y even after accounting for the difference in axis motion in the control. This may be explained by the cable mount's physical construction. As it consists of a helix of cable connecting two plates, it takes less force to move in the direction of the helix axis than it does to move any other direction orthogonal to the helix. The team hypothesized that if four cable mounts were used in a square orientation, the directional isolation difference would be reduced.

7.0 Conclusions:

Although the team didn't get data from the launch, the experiment was still a great experience. The issues found during the post-test analysis showed that more full system testing would have revealed these issues before the launch. These issues include the failure of the NXP / LPC board due to what the team thinks was improper handling, the lack of a pull up resistor on the active low chip select line causing one disconnect to propagate through the system, and the various software improvements that could be put in place to improve the reliability and performance of the system. The testing of a vibration isolation system is hard as the team did not have access to a proper vibration table. A vibration table capable of recreating the vibrations experienced during launch would make testing of the system significantly easier and improve the team's productivity.

Unforeseen circumstances occurred which caused our schedule to be delayed, and the implementation of the electronics and software of the payload was rushed. Should this project launch again, it is likely that the data acquisition system would take much less labor to develop, and many flaws found in this year's payload can be avoided. As most of the technical aspects of the data acquisition can be reused from this year's project, the team would have more resources to dedicate to the active system. In conclusion, the launch was not a success, but work done has successfully laid the work for future launches.

8.0 Potential Follow-on Work:

Projects looking to expand on this experiment could fully implement the active system which was left off the payload due to time constraints and lack of resources. The active vibration isolation component is complicated system that requires significantly more time and resources than the team was able to supply.

Another potential experimentation parameter would be changing how the passive damper material was in contact with the accelerometer. Last year's payload sandwiched the accelerometer between two pieces of passive material, while this year's payload had only one piece of passive material mounted on a single side with an adhesive. The placement of material around the accelerometer may change how vibrations penetrate the passive material.

Additional research can go into how vibrational energy effects various systems and what frequency ranges are the most dangerous to sensitive payloads. In short, there is more to be done in exploring this project.

9.0 Benefits to the Scientific Community:

The largest benefit to the scientific community would be the ability to use cheap, simple methods to reduce vibrations. Almost every craft launched into space contains sensitive sensors, equipment, and tools. Vibrations caused by the craft could skew sensor results or damage equipment. The project demonstrated multiple ways to reduce or eliminate vibrations in a cheap, effective manner. By expanding upon our research and experimentation, organizations seeking to launch spacecraft could design and subsequently include devices to reduce the vibrations experienced by sensitive equipment. This would save said organizations money and time, while allowing them to receive accurate results and avoid damage to equipment.

The results of this project could also be applied to any area where vibrations are a significant problem, since the methods detailed in this report are not only limited to spacecraft.

10.0 Lessons Learned:

The aims of this project were more ambitious than last year's launch -- two axis accelerometers, smooth active isolator motion, innovative magnetic system -- but proved to be less successful in terms of acquiring useful data. If the team decides to make next year's project as complicated as the current one, the amount of time and resources consumed must be taken into account. It was assumed that the current project would be less complicated because of the groundwork laid last year. This was not the case as the data acquisition system was designed from scratch. Another large time loss was the attempted use of store bought actuators which did not function as required. That choice essentially wasted all the planning phase of the project on a design that would not work. With the results of the tests performed after the launch, it is clear that earlier testing would have been useful in prior to launch rather than after the launch.

11.1 Appendices:

A1: Analysis Code - MATLAB plots for the post-launch analysis (modified from last year)

```
function main()
close all

input = csvread('out.csv');
neooffx=mean(input(:,6));
neooffy=mean(input(:,7));
contoffx=mean(input(:,2));
contoffy=mean(input(:,3));
cableoffx=mean(input(:,8));
cableoffy=mean(input(:,9));
mapsoffx=mean(input(:,10));
mapsoffy=mean(input(:,11));
```

```
neox=input(:,2)-neooffx;
neoy=input(:,3)-neooffy;
contx=input(:,6)-contoffx;
conty=input(:,7)-contoffy;
cablex=input(:,8)-cableoffx;
cabley=input(:,9)-cableoffy;
mapsx=input(:,10)-mapsoffx;
mapsy=input(:,11)-mapsoffy;

a1 = neox;
a2 = neoy;
a3 = contx;
a4 = conty;
a5 = cablex;
a6 = cabley;
a7 = mapsx;
a8 = mapsy;

range = 1:1332232;

times = linspace(range(1)/12350, range(end)/12350,length(range))';

% Figure 1: Power bar graphs


amp1 = trapz(times, abs(neox.^2));
amp2 = trapz(times, abs(neoy.^2));
amp3 = trapz(times, abs(contx.^2));
amp4 = trapz(times, abs(conty.^2));
amp5 = trapz(times, abs(cablex.^2));
amp6 = trapz(times, abs(cabley.^2));
amp7 = trapz(times, abs(mapsx.^2));
amp8 = trapz(times, abs(mapsy.^2));

labels = {'Neop X', 'Neop Y', 'Control X', 'Control Y', 'Cable X', 'Cable Y',
'MAPS X', 'MAPS Y'};

bar([amp1 amp2 amp3 amp4, amp5, amp6, amp7, amp8])
set(gca, 'XTick', 1:8, 'XTickLabel', labels);
ylabel('Relative Power')
title('Relative Power (area under AC waveform squared)')

save_fig('1')

figure;

% Figure 2: Raw data graph of region of interest

yscale = [-250 250];
```

```
xlab = 'Time since start (sec)';
ylab = 'Amplitude';
subplot(8,1,1);
plot(times, a1);
xlabel(xlab);
ylabel(ylab);
title(labels(1));
v=axis;
ylim(yscale);

subplot(8,1,2);
plot(times, a2);
xlabel(xlab);
ylabel(ylab);
title(labels(2));
axis(v);
ylim(yscale);

subplot(8,1,3);
plot(times, a3);
xlabel(xlab);
ylabel(ylab);
title(labels(3));
axis(v);
ylim(yscale);


subplot(8,1,4);
plot(times, a4);
xlabel(xlab);
ylabel(ylab);
title(labels(4));
ylim(yscale);

subplot(8,1,5);
plot(times, a5);
xlabel(xlab);
ylabel(ylab);
title(labels(5));
ylim(yscale);


subplot(8,1,6);
plot(times, a6);
xlabel(xlab);
ylabel(ylab);
title(labels(6));
ylim(yscale);
```

```
subplot(8,1,7);
plot(times, a7);
xlabel(xlab);
ylabel(ylab);
title(labels(7));
ylim(yscale);


subplot(8,1,8);
plot(times, a8);
xlabel(xlab);
ylabel(ylab);
title(labels(8));
ylim(yscale);


axis(v);

std_size()
save_fig('2')
figure

% Figure 6: Spectogram Graph over entire plot

%spectrogram(x,window,noverlap,f,fs)

subplot(8,1,1)
spectrogram(a1, 256, 60, 900, 12350, 'yaxis')
ca = caxis;
title(labels(1))

subplot(8,1,2)
spectrogram(a2, 256, 60, 900, 12350, 'yaxis')
ca = caxis;
title(labels(2))

subplot(8,1,3)
spectrogram(a3, 256, 60, 900, 12350, 'yaxis')
ca = caxis;
title(labels(3))

subplot(8,1,4)
spectrogram(a4, 256, 60, 900, 12350, 'yaxis')
ca = caxis;
title(labels(4))

subplot(8,1,5)
```

```
spectrogram(a5, 256, 60, 900, 12350, 'yaxis')
ca = caxis;
title(labels(5))

subplot(8,1,6)
spectrogram(a6, 256, 60, 900, 12350, 'yaxis')
ca = caxis;
title(labels(6))

subplot(8,1,7)
spectrogram(a7, 256, 60, 900, 12350, 'yaxis')
ca = caxis;
title(labels(7))

subplot(8,1,8)
spectrogram(a8, 256, 60, 900, 12350, 'yaxis')
ca = caxis;
title(labels(8))



std_size()
save_fig('6')

end

function std_size()
      set(gcf, 'Position', [1000, 400, 850, 800])
end

function save_fig(name)
 print(name,'-dpng')
end

function plotthing(thing,number)
      subplot(4,1,number);
    plot(linspace(0,length(thing)/12350, length(thing)), thing);
      ylabel('Amplitude')
      xlabel('Time (sec)')
end

function fftplot(x, name, number)
subplot(4,1,number);
Fs = 12350;
t = 0:1/Fs:1-(1/Fs);
xdft = (1/length(x))*fft(x);
freq = -12350:(Fs/length(x)):12350-(Fs/length(x));
out = abs(fftshift(xdft));
plot(freq(int64(length(freq)/2):end),out(int64(length(out)/2):end));
```

```
set(gca, 'XTick',...
      0:4000:22000,...
      'XTickLabel',...
      arrayfun(@(x) sprintf('%d kHz',x), 0:4:22, 'UniformOutput', false));

title(strcat(name, ' FFT over 3 second region'))
xlabel('Freqency (kHz)')
ylabel('Amplitude')
ylim([0 0.004]);
end
```

A2: Schematics for Accelerometer Breakout Boards

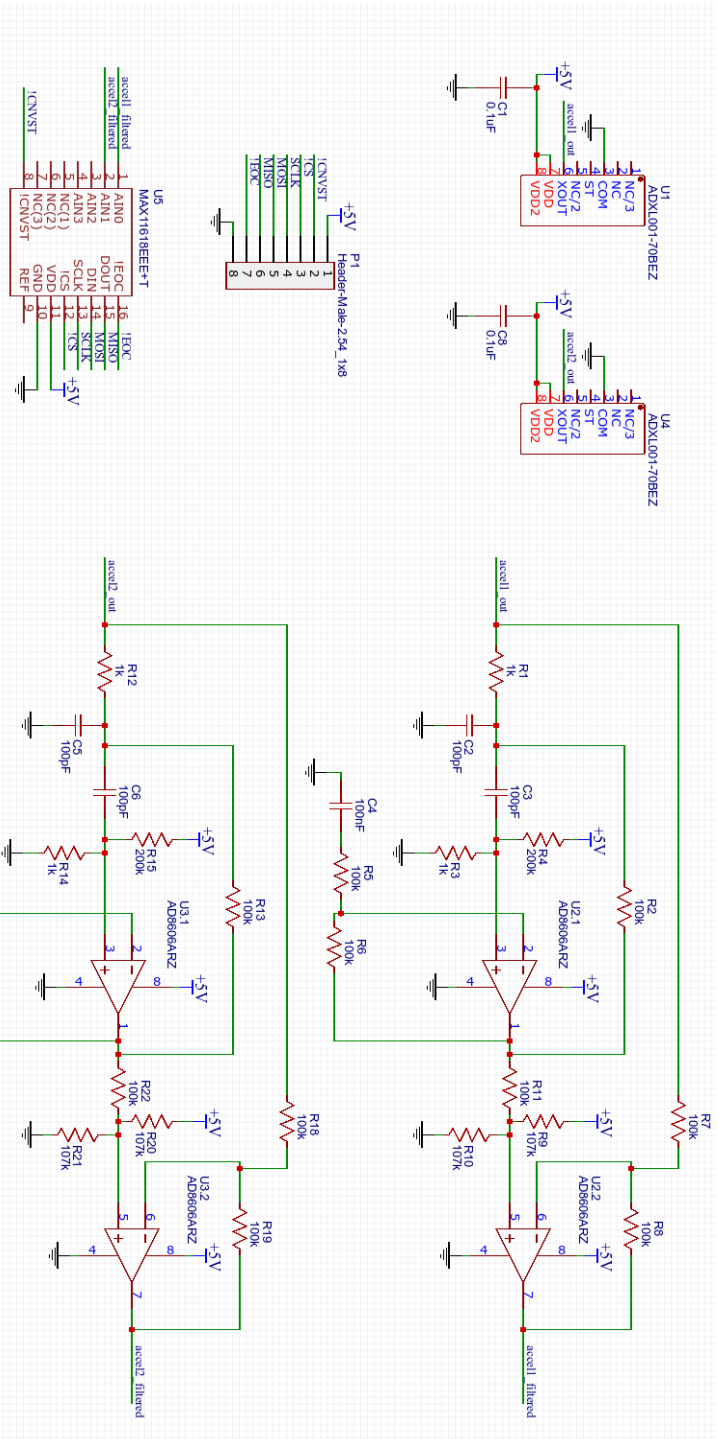
U1
ADXL001-70BEZ
U4
ADXL001-70BEZ
U5
MAX11618EEE+T
P1
Header-Male-2.54_1x8
U2.1
AD8606ARZ
U2.2
AD8606ARZ
U3.1
AD8606ARZ
U3.2
AD8606ARZ
accel1_out
accel2_out
accel1_filtered
accel2_filtered
!CNVST
+5V

A3: Layout for Accelerometer Breakout Board

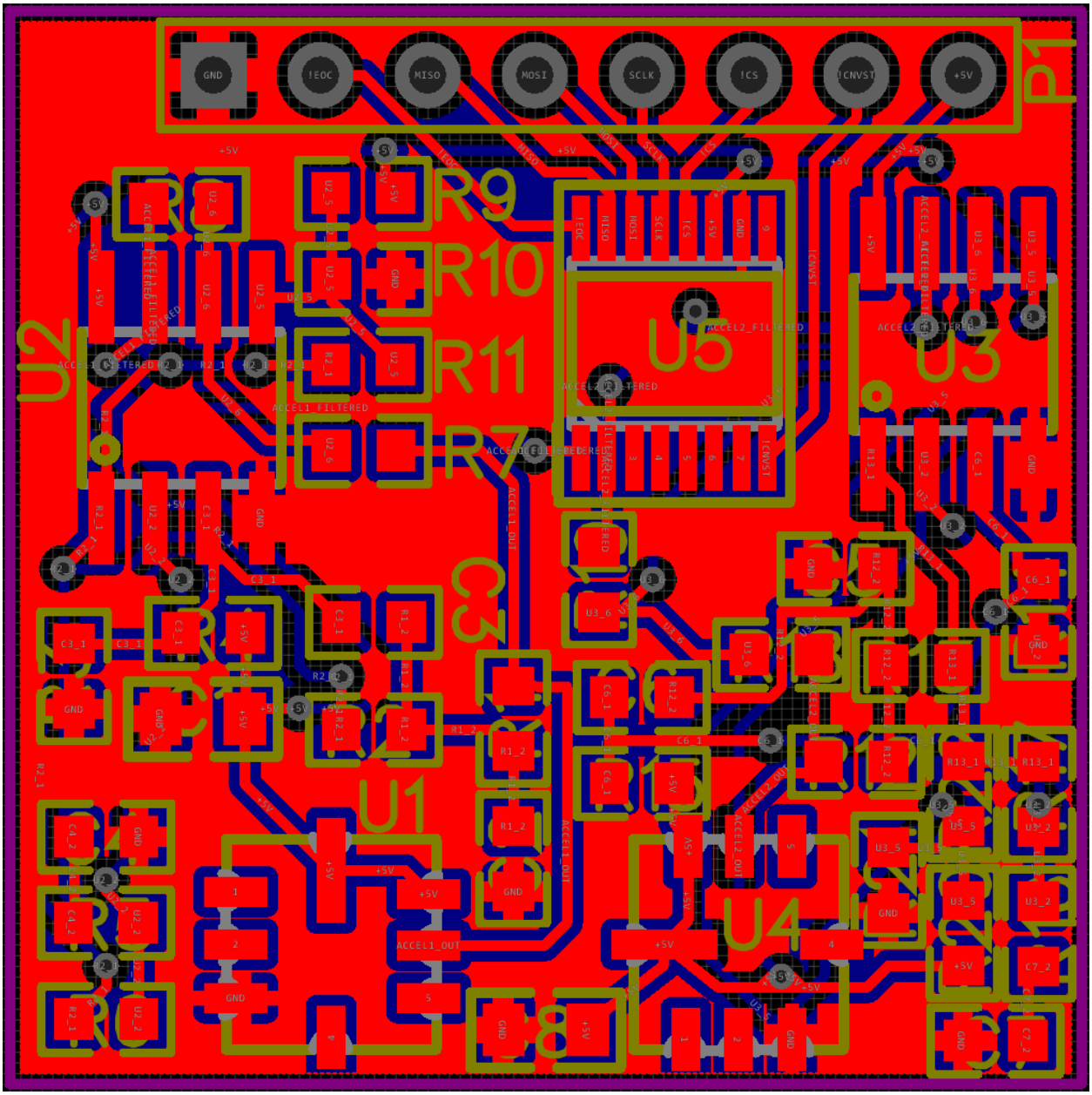

A4: Schematic of the Motherboard

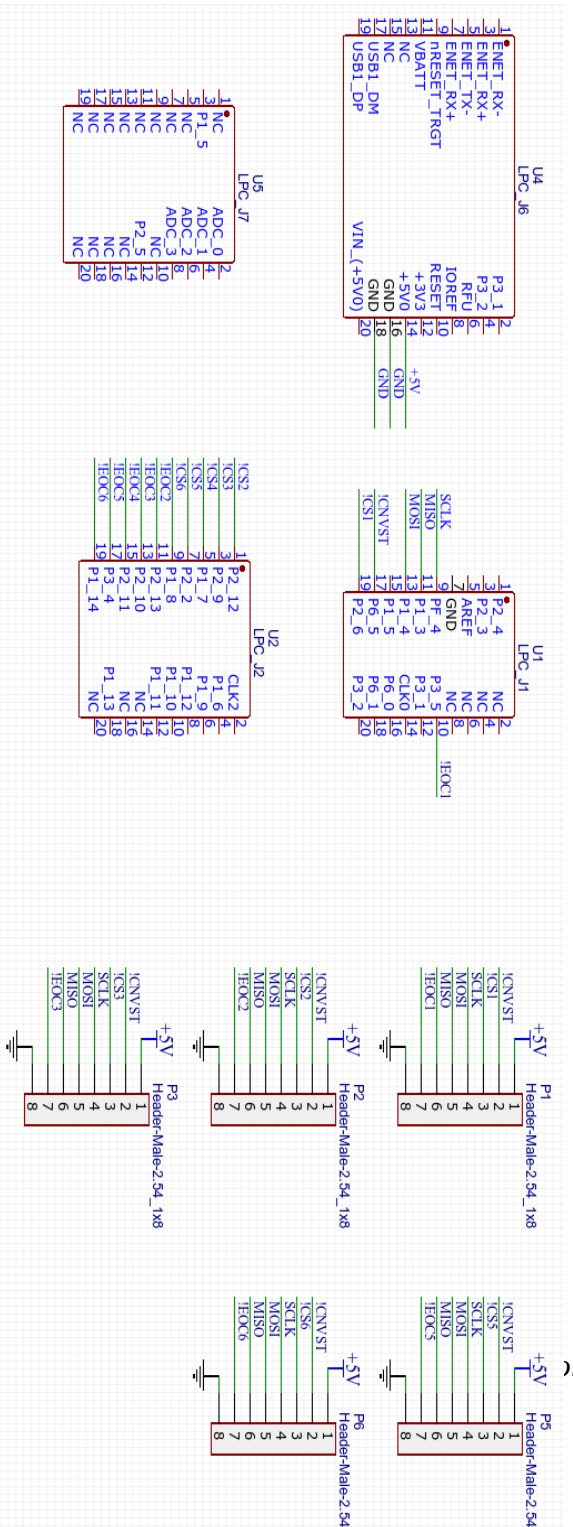
U4
LPC_J6
ENET_RX-
ENET_RX+
ENET_TX-
ENET_RX+
nRESET_TRGT
VBATT
NC
NC
USB1_DM
USB1_DP
P3_1
P3_2
RFU
IOREF
RESET
+3V3
+5V0
GND
GND
GND
VIN_(+5V0)
+5V
GND
GND
U5
LPC_J7
NC
P1_5
ADC_0
ADC_1
ADC_2
ADC_3
U2
LPC_J2
P2_12
P2_9
P1_7
P2_2
P1_8
P2_13
P2_10
P2_11
P3_4
P1_14
CLK2
P1_6
P1_9
P1_12
P1_10
P1_11
U1
LPC_J1
P2_4
P2_3
AREF
GND
PF_4
P1_3
P1_4
P1_5
P6_5
P2_6
SCLK
MISO
MOSI
!CNVST
!CS1
NC
P3_5
P3_1
CLK0
P6_0
P6_1
P3_2
!EOC1
P1
Header-Male-2.54_1x8
P2
Header-Male-2.54_1x8
P3
Header-Male-2.54_1x8
P5
Header-Male-2.54
P6
Header-Male-2.54
+5V
!CNVST
!CS1
!CS2
!CS3
!CS5
!CS6
SCLK
MOSI
MISO
!EOC1
!EOC2
!EOC3
!EOC5
!EOC6

A5: Layout of the Motherboard

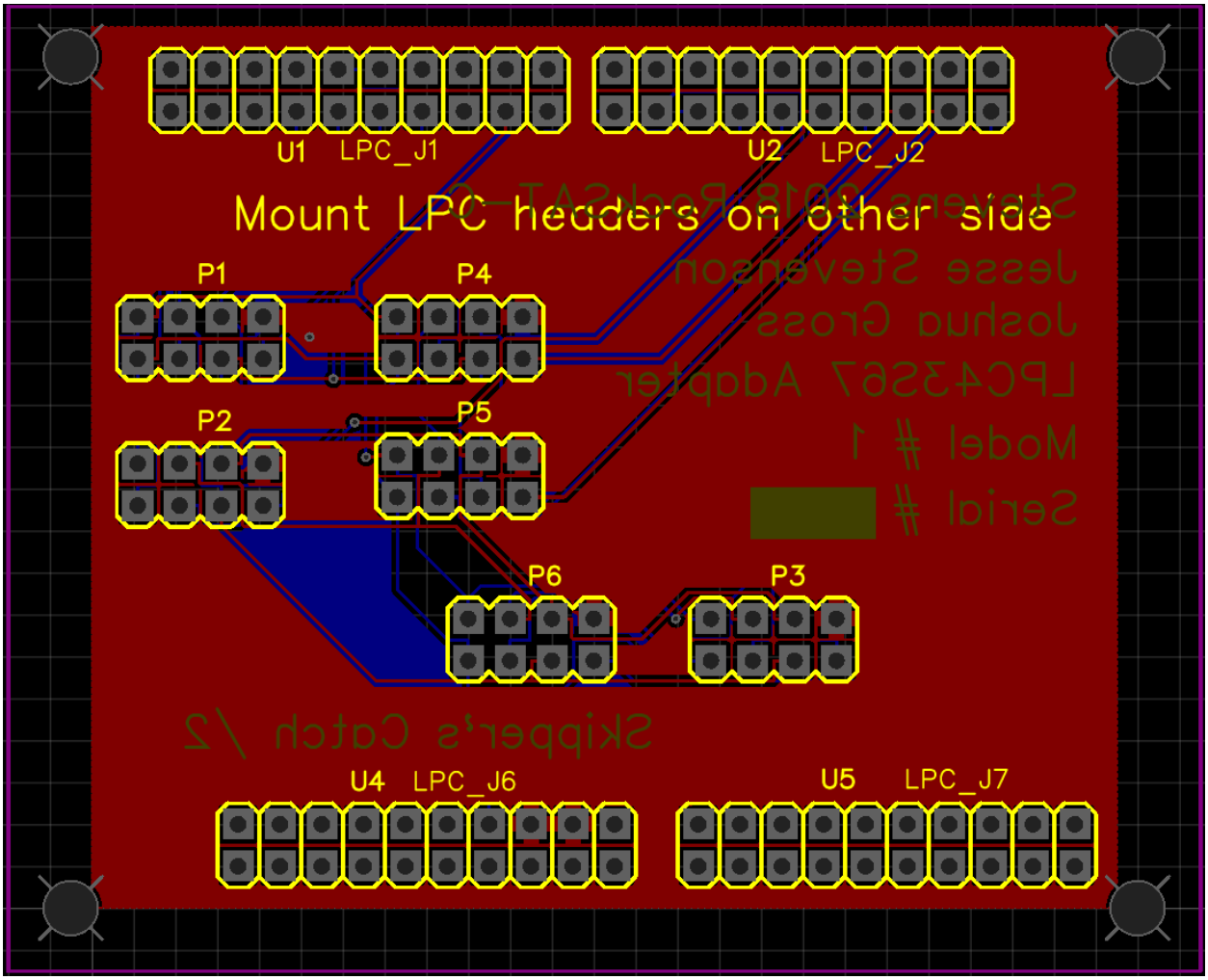

A6: Microcontroller / Linux code - on GitHub at https://github.com/Stevens-RockSAT-2018

Part 2: Pressure Sensor

1.0 Mission Statement:

The goal of this project was to record and analyze high-speed aerodynamic phenomena that occur at high-speed vehicles, such as rockets, at velocities of Mach 4 and above. The mission of this year's iteration of the Pressure Sensor project was to expand upon the previous year's attempt by making the system more modular, more mechanically robust, and to improve the software to enhance the sampling rate of the digital sampling subsystem. To accomplish this, multiple strategies were used, such extensive use of PCB design to create a compact and reusable system, as well as utilizing an existing open-sourced Data Acquisition Unit (DAQ) to expedite the development process. The team expected to learn more about the aerodynamic phenomena of boundary-layer transitions, as well as the engineering process of designing high-performance analog and digital circuitry.

2.0 Mission Requirements and Description:

As high-speed vehicles such as rockets approach speeds on the order of Mach 4, a boundary-layer transition is expected to occur on the interface of the rocket skin and the surrounding atmosphere. To better understand this, consider a rocket cutting through the atmosphere at high speeds. Directly on the outside of the rocket skin, there lies a film of air that "hugs" the skin of the rocket and moves at a velocity very close to the velocity of the rocket. Much further away from the rocket skin, there is the relatively stationary atmospheric air. Somewhere between these two streams of air, there is a "boundary layer" where these air streams must interact - this we will call the interface. When the velocity of the rocket becomes sufficiently high, these two air streams will begin to act very chaotically at the interface, as the high speed air tends to "rip" away at the low speed air, which at a macroscopic scale contributes to the friction known as air resistance. At a much smaller scale, however, there are expected to be high-frequency acoustic noises produced at this junction. The pressure teams set out this year to analyze the nature of this acoustic energy.

First, before the DAQ was designed to collect data, the team collected as much information as possible about the nature of these oscillations. With the guidance of Professor Nick Parziale, it was determined that the characteristics of the noise radiation are as follows:

Amplitude: 0 - 100 Pa Peak-Peak
Frequency: 0 Hz - 1 MHz

In order to digitally sample analog signals up to 1 MHz, it was required by Nyquist's Sampling Theorem to sample at 2 MS/s or greater. The system must have sufficient analog signal gain to capture the 100 Pa peak-peak signal with good dynamic range. Other mission requirements were

that the unit must sample for at least 10 minutes duration in order to ensure that the launch window is not missed.

These real requirements were then translated into the Technical Design Requirements (TDR):

1. Analog subsystem must have analog gain of 1000 (30 dB).
2. Digital sampling subsystem must have a sample rate of at least 2 MS/s.
3. Digital Sampling subsystem must have enough memory to hold 10 minutes of sampling
    a. 2 Megasamples/second x 10 minutes x 2 bytes/sample = 2.4 GB of non-volatile memory
4. System must contain all power regulation electronics to power the analog signal conditioner board, as well as digital sampling subsystem

Once these key parameters were understood, the team procedure to designing the payload.

3.0 Payload Design:

In order to improve upon last year's payload, which was plagued with mechanical integrity problems, much foresight was given to making this system mechanically and electrically robust. The BeagleBone Black microcomputer was chosen as a processing unit. To expedite the development process, the work of the Google Project called PRUDAQ, an open source high-speed sampling system designed for the Beaglebone, was leveraged. The PRUDAQ system is a cape which interfaces with the Beaglebone with sturdy pin headers. This was utilized to create the **Digital Sampling Subsystem.**

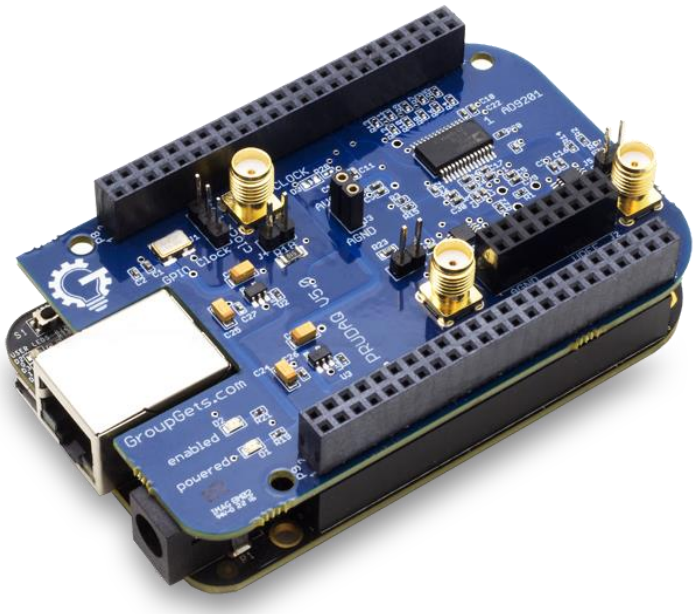

Figure 1. PRUDAQ Cape mounted to Beaglebone Black (Image credit: Google)

The PRUDAQ contains a 10-bit Analog to Digital converter (ADC) which accepts a 0-2 volt analog input on 8 different channels. For the purposes of this project, only one of these channels was used. In theory, this ADC is capable of producing enough samples for 40 MS/s sampling rate, which is fast enough to make a software-defined radio (SDR). However, because of limitations in non-volatile memory speeds, it is very difficult to shuffle this much data into memory as quickly as it is produced. Even at sample rates of 2 MS/s, the team in previous years was unable to move 2 MS/s worth of data into memory without the loss of data. Because the PRUDAQ project has a great software package which can accomplish the speeds the Pressure team was looking for, it was decided to use this cape. While the team did wish to learn more about the design of high-speed digital electronics, there were other important system components to design, such as the analog signal conditioning section.

The next major subsystem onboard was the **Analog Signal Conditioner Board.** This PCB was custom designed in EAGLE CAD by team member Chris Blackwood, and constituted a significant portion of the work done on this project. The board is shown below:

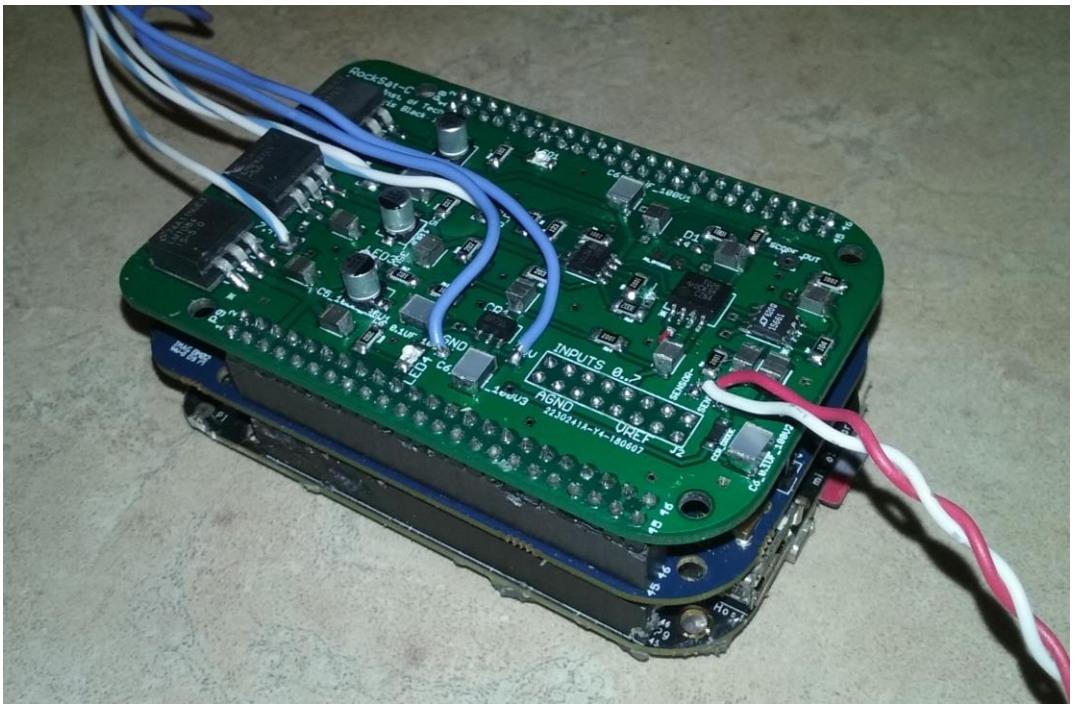

Figure 2: Custom Signal Conditioner Board stacked onto PRUDAQ and Beaglebone

The signal conditioner board contains 4 voltage regulators which accept unregulated power from the LiPo batteries onboard the canister. There is a 5-volt digital rail to power the Beaglebone and PRUDAQ, the power for which gets routed down through the header pins. There are 5 and 10 volt analog rails for the analog electronics which includes Op Amps and a low-pass filter. Lastly, there is a 24-volt analog rail to power the pressure sensor itself via a constant-current source. The schematic for the signal conditioner was first drawn out by hand, then translated into CAD. See the appendix for the schematics and PCB layout for the Signal Conditioner Board.

The signal conditioner board was required to have a low-pass filter with a cut-off frequency of 2.3 MHz, since the Digital Sampling Subsystem was at one point slated to sample at 5 MHz. Due to test results found later in the *Testing subsection*, the team was unable to get the Beaglebone to accept data from the PRUDAQ at a rate faster than about 223 kS/s. Despite this digital sampling system difficulty, the signal conditioner's cutoff frequency was kept at 2.3 MHz due to the lack of time reserved to make signal conditioner board revisions.

The board also features a multi-stage amplifier to provide 30 dB of total system gain. The low pass filter IC provides 12 dB of gain in the passband, and two additional op amps provide the remainder of the gain. One special feature of this gain setup is the use of an op amp with an Automatic Gain Control pin. This pin accepts an analog voltage input which comes from an envelope detector circuit. The purpose of the Automatic Gain Control circuit is to tailor the gain to maintain a relatively constant amplitude at the Analog to Digital Converter (ADC) input. This serves two purposes: because the amplitude of the acoustic phenomena is not well established, the team had to make some guesses as to the amount of gain required in the system. The AGC circuit provides flexibility in this regard, as the circuit can collect distortion-free data over a wider range of input amplitudes. Additionally, it maximizes the dynamic range of the ADC, ensuring that the input voltage to the ADC is from 0-2 volts DC. If the signal were too small, the ADC would have very poor resolution in measuring the signal; in contrast if the signal were too big, the signal would be very distorted. The AGC function mitigates the impact of these two scenarios.

Software

On the software side, the Beaglebone OS is linux and most real-time functionality was provided via the open-source software BeagleLogic. This system image provided interfacing between the beaglebone and PRUDAQ without impinging on any of the high speed capabilities of the PRUDAQ. In order to accomplish our mission goals as shown below, we had to efficiently employ BeagleLogic.

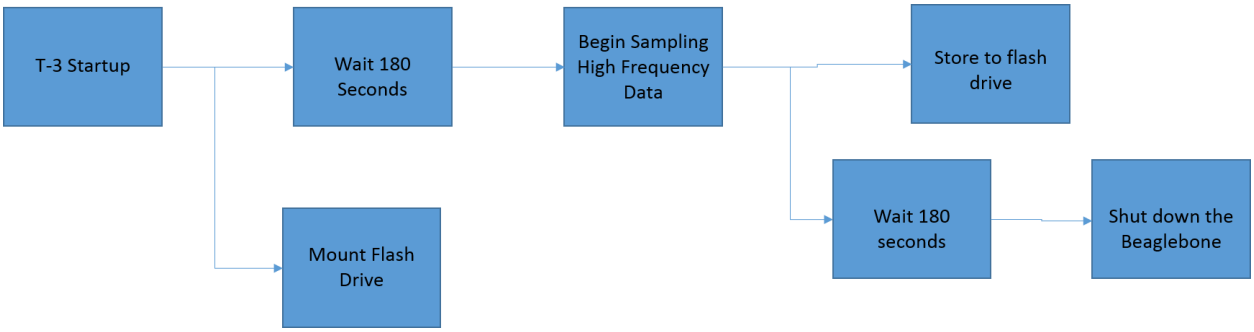

Figure 3: Software Flow Diagram

The bulk of the final software, which needed to be concise to maintain high speed constraints and minimize buffer overflow and therefore data loss, ended up being one line:

stdbuf -oL hexdump -d /dev/beaglelogic >> {Flash Drive File Path}

Hexdump -d /dev/beaglelogic is software provided by Beaglelogic which dumps data being stored in a temporary buffer bin in the file location /dev/beaglelogic. This command outputs a constant stream of data to stdout which can be viewed through the command line output. Because this data is being output to stdout, it can then be rerouted to via the >> operators which suppress the command line output and route the data to a text file within the SD card. The double > operator indicates the append mode as opposed to the overwrite mode. Furthermore, the rerouting of data can only occur once the stream has ceased. Because the hexdump streams continuously, the *stdbuf -oL* command creates a buffer between each line (-*L*) of the output (-*o*) which allows each line to be appended to the file in the SD card.

The one line above constitutes the main functionality of the software. To implement this and the other tasks (SD mounting, timing, and system kill), a short c-script was written and compiled into an executable which was then added to a startup bash script that runs when the beaglebone turns on with the T-3 switch.

Aside from the internal components of the payload, a port pocket window was designed to house the sensor. The pressure sensor is essentially a short metal tube with a diaphragm on the end. It is designed to be mounted using silicone on the side walls in the housing hole. To prepare for this a multi-purpose port cover was designed based off of the original cover provided. The window was designed with four countersunk holes for mounting to the port pocket and a center through hole for the sensor. After using CAD to create a model and produce G-code for machining, the cover was machined on a prolight CNC. The final window cover is shown below with the sensor mounted.

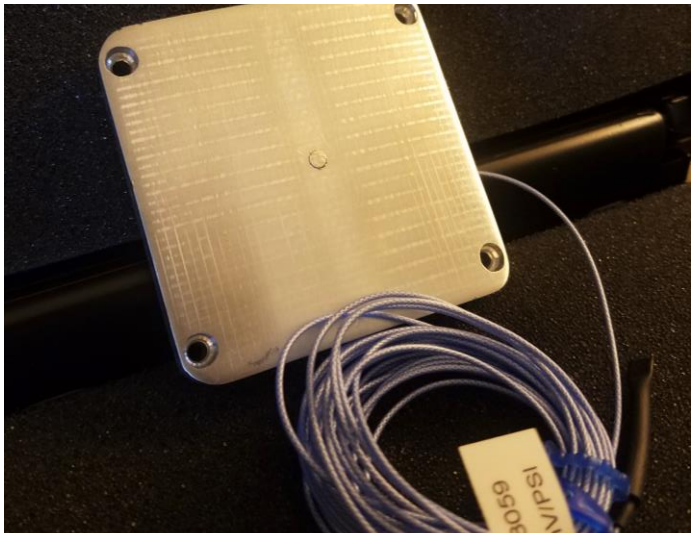

Figure 4: Port Window with Pressure Sensor Installed

Power Distribution Board

Due to the variety of different power rails present on the payload, it was not possible to use only one activation line to activate the payload. Instead, the signal from the activation line was used to drive a power distribution board, which used power MOSFETs to switch the load on and off. This board is used for both the Pressure Team as well as the Vibration Team, with 3

MOSFETs for the Pressure team, and 1 MOSFET for the Vibration Team. The circuit uses NPN transistors at the gate of the P-Channel MOSFETs to provide logic inversion as well as gate isolation so that all four gates can be controlled by the same activation line.

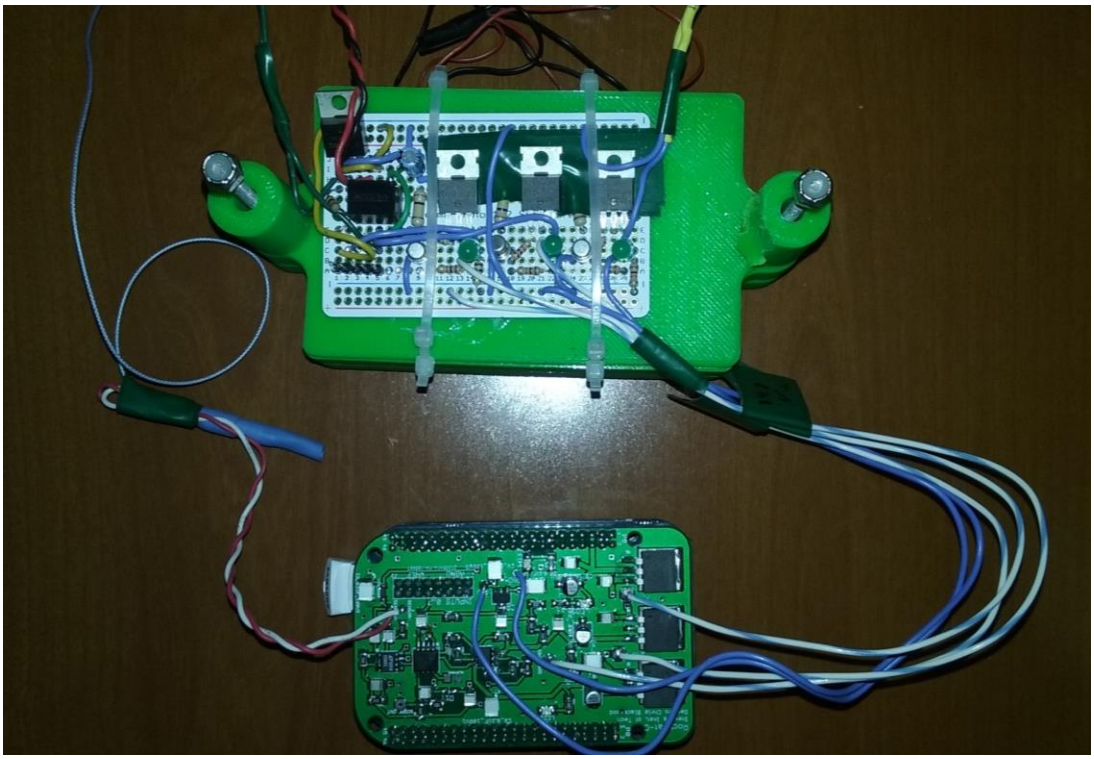

Figure 5: Power Distribution Board, feeding power into the Pressure Team's electronics

The block diagram below illustrates how the power distribution board switches power from the batteries to the payload.

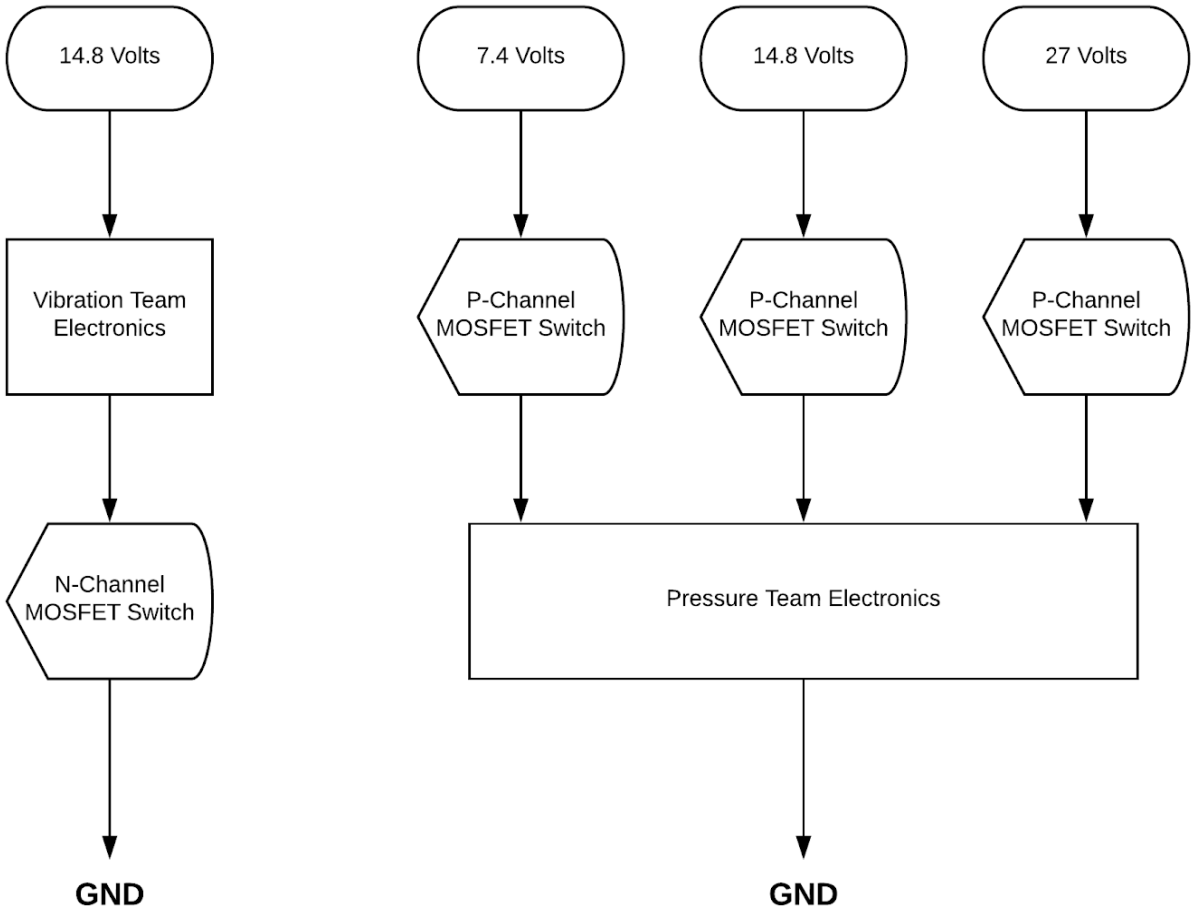

Figure 6: Power Distribution Board Block Diagram

The specific details of the Power Distribution Board's functionality as well as pitfalls are explained in more detail in Section 6, Mission Results, as these details are more relevant in that discussion.

4.0 Student Involvement:

The following members contributed to the completion of this project:
Chris Blackwood - Electrical Design of Signal Conditioner PCB and Power Distribution Board
Chris Cowan - Software Development, Payload Integration, Design/Construction of port window
Alex Austin - Presenter and Project Timeline
Ronald Ankner Jr. - Software Development
Richard Thornton - Systems Engineering

5.0 Testing Results:

The digital sampling subsystem was the first system to undergo testing, as it consists of only the Beaglebone Black and the PRUDAQ, which are off-the-shelf boards. Preliminary code was written to test the sampling ability of the PRUDAQ and to ensure that the system code mount the USB Flash drive and write data successfully.

The Analog Signal Conditioner board underwent two different phases of testing. First, however, the build process for the PCB will be documented here. For the first iteration of the board, the signal conditioner PCB was etched manually using the toner transfer method, and was etched with Ferric Chloride acid.

Figure 7. A copper-clad fiberglass board is run under a hot laminator to transfer the PCB design onto the copper.

In the interest of accelerating the build process (as the deadline was quickly approaching at this moment in time), the team sought out to manually etch the PCB while the professionally manufactured PCBs were being made. A double-sided copper clad board was used as the substrate, and was cleaned thoroughly with acetone and Scotchbrite pad to remove any residues and oxidation from the copper. The PCB design was printed onto HP Presentation Paper with a Laserjet printer (not to be confused with inkjet).

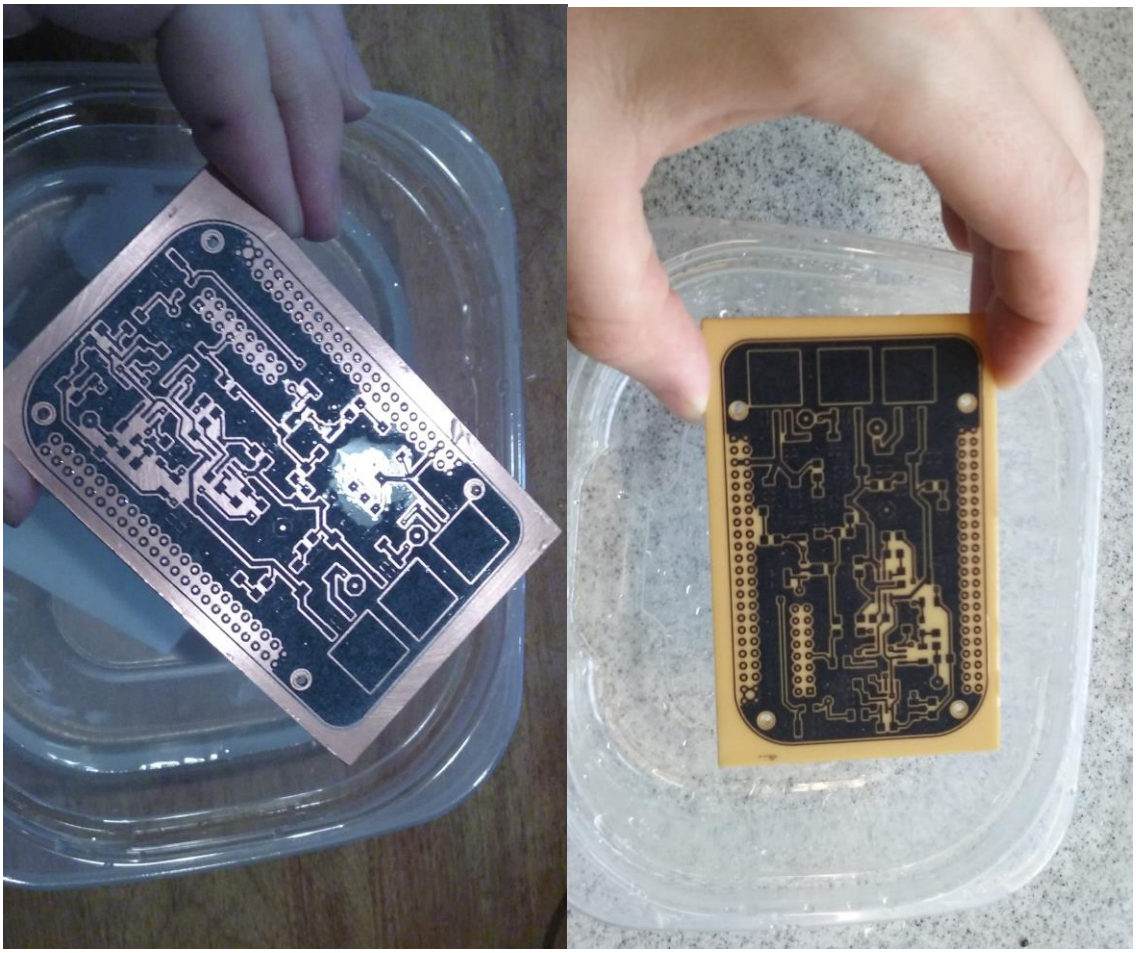

Figure 8 and 9. On the left: The PCB after toner was transferred onto the copper, and the backing paper was peeled off under water. On right: The PCB after etching in a ferric chloride acid bath (FeCl3), and rinsed with water.

Multiple papers were tried, including glossy photo paper; this was found to leave a plastic residue on the copper board. Presentation Paper is slightly glossy yet is not quite plastic; of the papers tested, it was found to be the best paper used for the Toner Transfer Method, as it transfers cleanly and peels away easily later when soaked with water.

The board was etched in warm Ferric Chloride acid, which was warmed on a hotplate. The FeCl3 was used in a plastic container which floated on a warm bath of water in a metal pot. As a word of caution, Ferric Chloride may seem to be a rather timid acid - but when warmed, the vapors are *quite nasty!* Team member Chris Blackwood remarked that despite wearing large rubber gloves and chemical goggles, the vapors irritated his nose and eyes. If one chooses to etch a board using this method, use a fume hood, and keep the temperatures low. Ferric Chloride need only be slightly above room temperature to work sufficiently fast. It is better to have a slow etch than to risk inhaling toxic vapors.

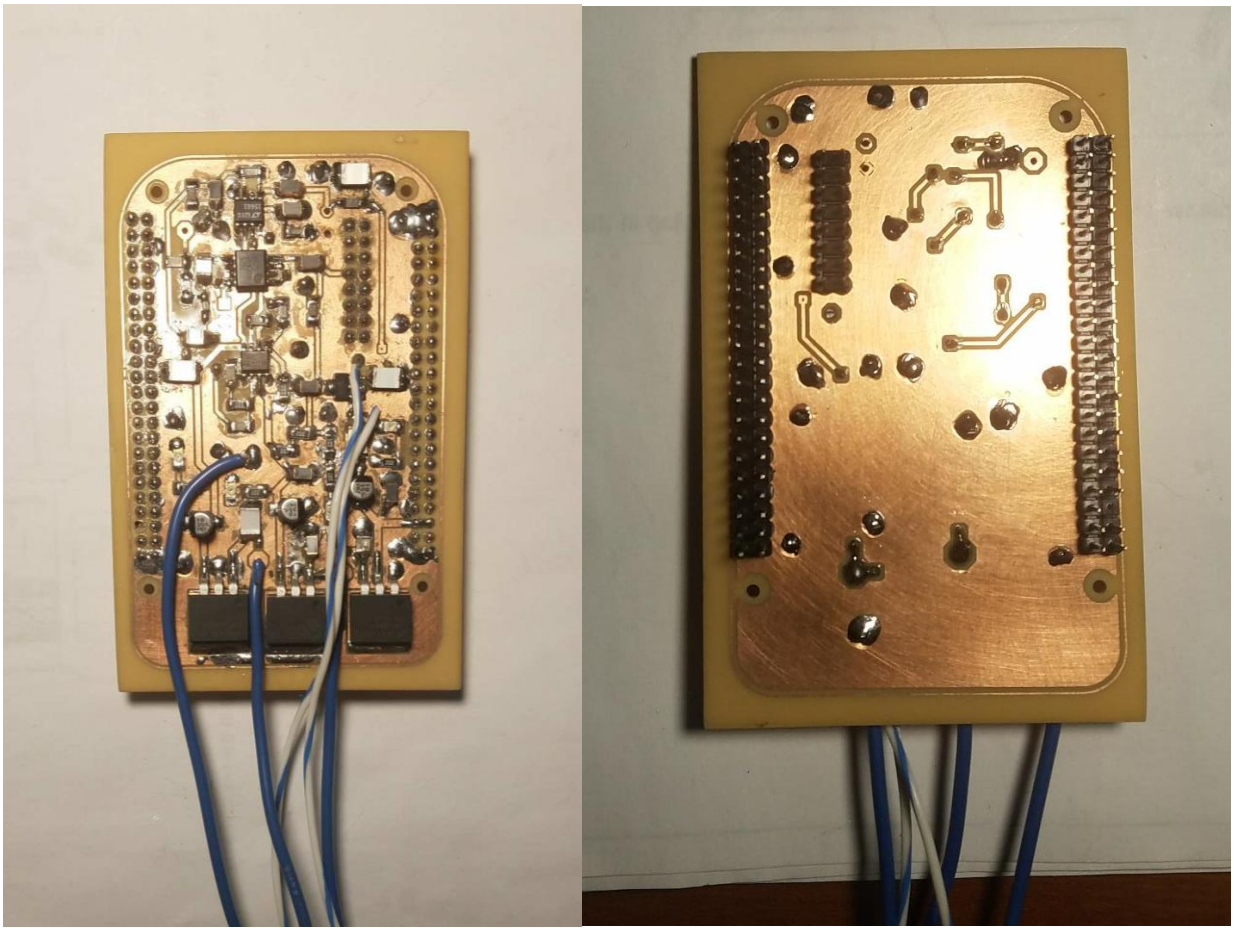

Figures 10 and 11: On left: Soldered PCB, top side. Right: Bottom side of board. Notice the pin headers which interface with the PRUDAQ.

The board was then drilled using very small carbide tipped drill bits. Vias were handmade by soldering small wires from one side to the other through the holes. The process of etching, drilling, and assembly took an incredible amount of time, on the order of 10 to 12 hours total for an experienced worker.

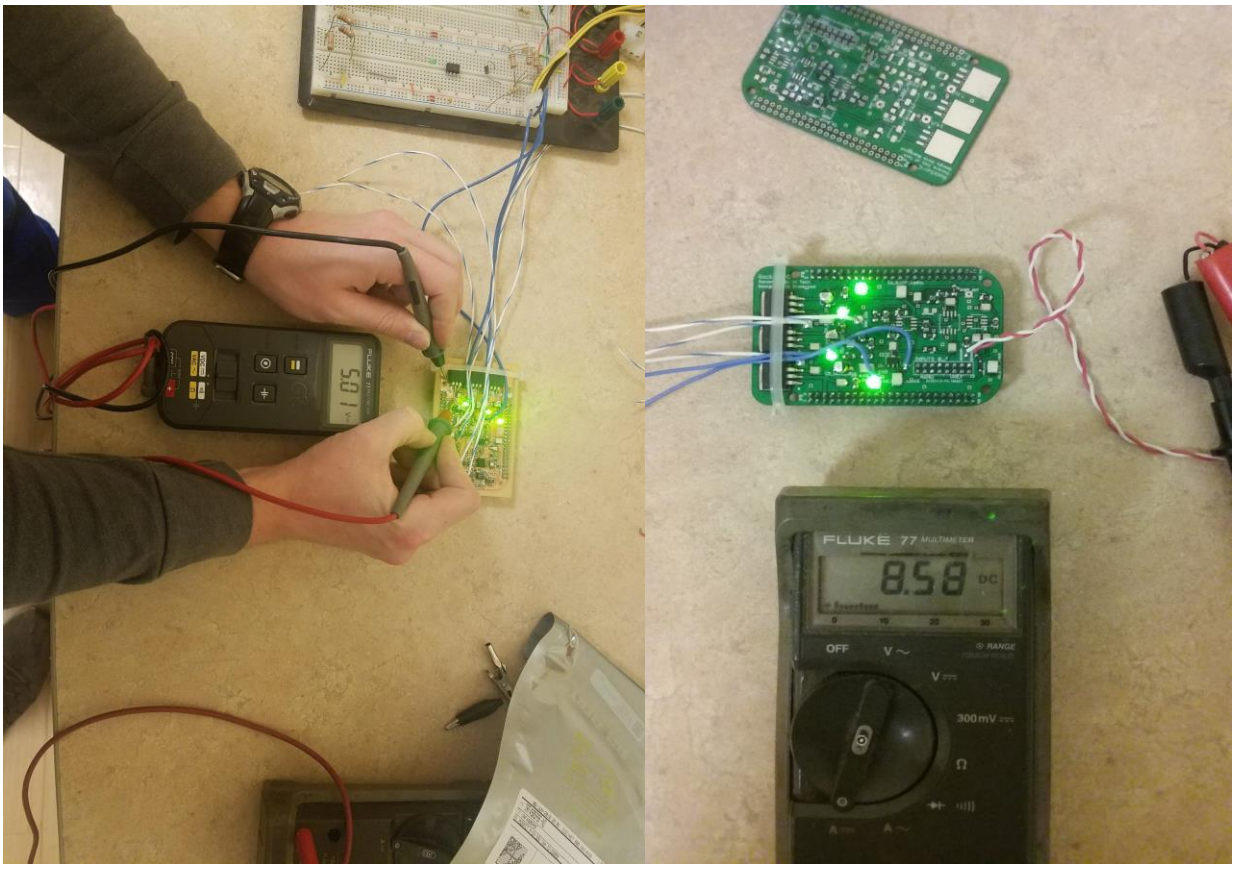

Figures 12 and 13. Left: Testing the voltage regulators on the home-etched PCB. On right: testing the sensor excitation current output on the professionally etched PCB, with the multimeter reading an output current of 8.58 mA. Both boards behave identically, but the professionally etched board affords a higher degree of confidence in the mechanical integrity under vibration stresses.

The handmade board was tested, as well as the professionally fabricated PCB (which was also hand-soldered). Both boards met the testing criteria for DC analysis; the onboard power supplies worked as expected. One interesting observation was made: the power regulators were tested before the large decoupling capacitors were installed. Without the stabilization afford by the capacitors, the voltage regulators engaged in oscillations, which actually made them fail to regulate and instead output full input voltage! In other words, the 5 volt regulator was outputting close to 12 volts due to oscillations stemming from the lack of proper decoupling capacitors. When proper decoupling capacitors were installed, the power supplies began operating properly and steadily.

AC Analysis of Signal Conditioner Board

The boards were also tested for their ability to properly amplify at the input signal. A small AC input voltage from a signal generator was input in the sensor input, and the voltage output to the PRUDAQ was measured using an oscilloscope. It was found that while the circuit

contains multiple gains stages, as well as an automatic gain control circuit to adjust the gain according to the input amplitude, only one gain stage worked properly. This stage provided a gain of 12 dB, which was much lower than our original required gain of 30 dB. Despite this, little time remained to fix the nonfunctional automatic gain control circuitry, so this circuitry was bypassed. The total system gain for the final payload was 12 dB, which may or may not have been sufficient. Because the team does not truly know the real amplitude of the acoustic radiation to be measured, it is yet unknown whether or not 30 dB is truly necessary.

The results of the testing are summarized below:

1. **Voltage Regulation: Pass**
2. **Analog Signal Gain: 12 dB (Partial failure, original required gain: 30 dB)**
3. **Sensor Excitation Current: 8.58 mA (Pass, required current per sensor specification: 5 mA - 20 mA)**

Digital Subsystem Testing

The digital subsystem was tested using the Beaglebone Black paired with the PRUDAQ cape. The test included three main criteria:

1. The digital sampling subsystem must be able to record data at a rate of 2 MS/s.
2. The system must accurately convert analog inputs to digital samples of 10-bit resolution.
3. The system must store the data in an onboard USB flash drive.

The results of the testing were as follows:

1. **Sampling Rate: 223 kS/s (Fail, expected value: 2 MS/s)**
2. **Accuracy of conversion: Pass**
3. **Data storage: Pass, successful write to USB Flash Drive**

While the digital sampling subsystem did perform the elementary functions of collecting data and storing it onto the non-volatile memory, the rate at which it collected data was determined to be 223 kS/s, which is approximately one-tenth of the desired value. The team suspects that this bottleneck is the result of the use of STDOUT to write the information stream to the file, which likely required extra memory overhead in the central processor to properly write the information. This function should have been performed by the Programmable Real Time Unit (PRU) onboard the PRUDAQ. It is quite likely that the team did not properly implement the PRUDAQ software library, as the original designers of the PRUDAQ were able to achieve sample rates up to 20 MS/s per channel with the same setup (Beaglebone Black, PRUDAQ, and the same Samsung 64 GB, USB 3.0 Flash Drive).

Despite the subpar sampling rate, the time decided to move forward with the Digital Sampling Subsystem in order to spend more time on other systems such as the Power Distribution Board and the Signal Conditioner Board. Without these other systems, the entire DAQ would not be functional; so it was decided to bring all systems to a mostly-working state,

then fix non-functional features later. Unfortunately, the team did not have enough time to fix these issues (inadequate sampling rate and non-functional Automatic Gain Control circuit), so the payload was launched as-is. As it turned out, these problems were relatively small in comparison to what happened next.

6.0 Mission Results:

When the payload was received after launch, the team was very careful to ensure that the activation line on the payload was not accidentally turned on. While the code was written in such a way as to append additional data to the existing text file without overwriting any information, it was decided that it would be best to keep any accidental turn-ons to a minimum. The SD Card, which contains the boot disk for the Beaglebone, was unplugged first, and the flash drive, which was expected to contain data, was unplugged second. Much to our surprise, the flash drive did not contain any files - it was completely blank upon recovery, which indicates that a failure did occur with either the electrical or the software systems onboard the payload.

Failure Analysis

Before any major failure analysis was performed, the SD card was first copied to create a backup image in case the original image got corrupted in our testing process. The team wanted to remove any variability that would compromise the confidence in our post-launch analysis. Furthermore, no glaring electrical issues could be found with the system - all power regulators were producing the correct voltages and were not overheating, which could have indicated a short circuit somewhere on one of the boards. The team eventually determined that the Beaglebone used in the launch failed to boot entirely. It was first suspected that the SD card had become corrupted somehow, which caused a complete failure to boot upon launch.

In order to rule out what might have caused the boot issue, the team got its hands on a second Beaglebone known to work properly. The Beaglebone was loaded with the SD card used at launch, and voila - the second Beaglebone booted properly! From this test it was determined that the SD card was not corrupted, but it was the Beaglebone Black used at launch that was entirely dead. Power LEDs would turn on to indicate that the 5V digital power supply turned on, but no boot lights would blink as they should have.

What caused the Beaglebone to become fried before the launch?

This much is known: before the final check-in, which is the last opportunity to make any changes whatsoever to the payload, we know that the Beaglebone functioned properly, as the software was being tested 2 hours before final check-in. The issue must have occurred in the final two hours when the Vibration Team, who was in charge of payload integration and assembly, was given the payload to assemble.

One known incident which occurred, which most likely fried the Beaglebone, was when

the Pressure Team electronics were being assembled to the Lexan mounting plate. Both team's payloads were mounted on opposite sides of the Lexan plate using the same bolt-holes. A long metal bolt ran through the Pressure Team's 3 board stack, into the Lexan Plate, then through the Vibration Team's electronics board. The mechanical engineer in charge of mounting these components was not aware that in doing so an electrical connection was formed across both systems (as the metal bolts contacted the metal ground-pour on the Beaglebone PCB and the Vibration Team's PCB). **Normally this should not be an issue, but because of the manner in which the Power Distribution Board switches the two loads, there is a potential difference between the ground planes of the two systems!** When the two boards were connected, the Vibration team noticed that both payloads suddenly turned on while the activation line was off, and quickly found another mounting solution to prevent this. Their solution was to electrically isolate both systems by using separate mounting bolts. Little did we know, the damage had already been done, and our Beaglebone was most likely fried due to a reverse-voltage scenario which occurred as a result. The following diagram helps to explain the mode of failure specifically - it has already been shown in Section 3, Payload Design, but it has been shown again here for reference:

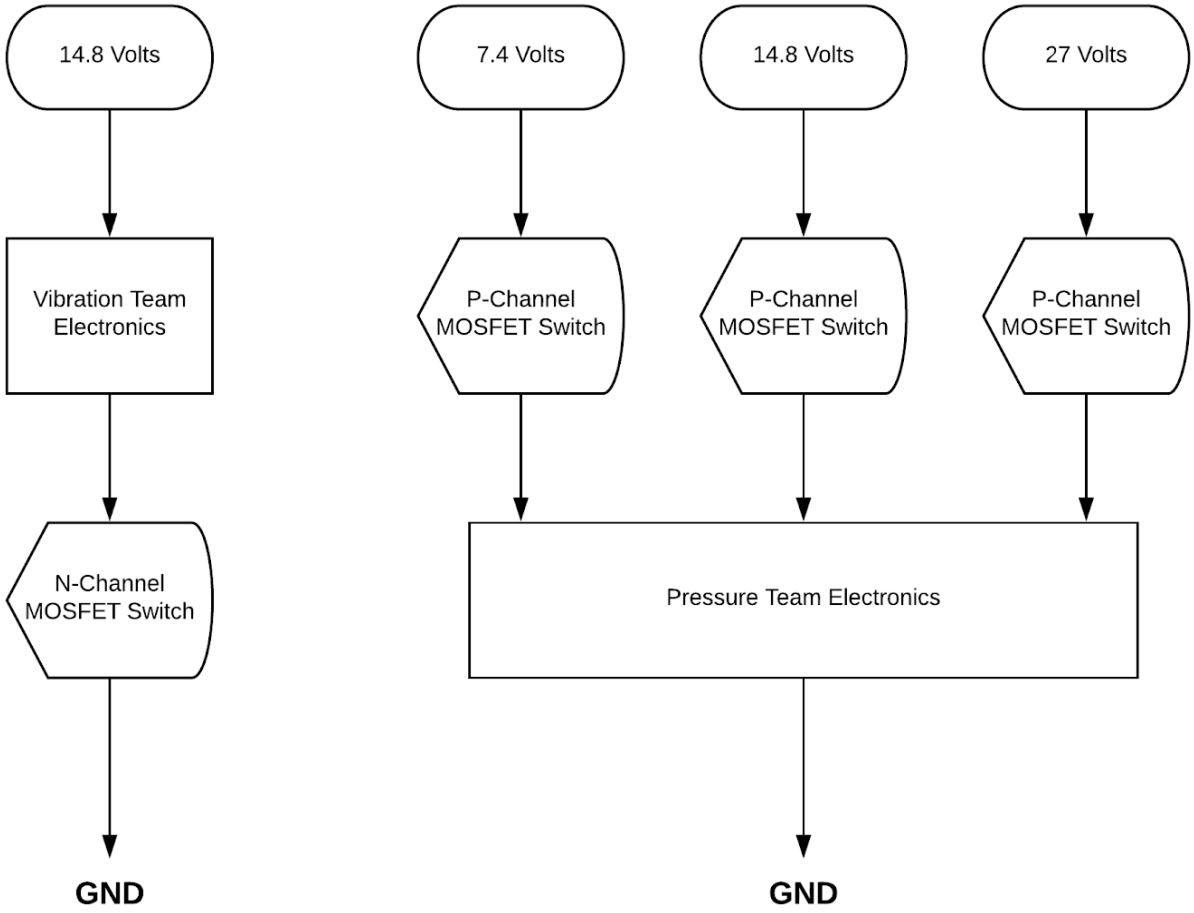

Figure 14: Power Distribution Board Block Diagram

In the above diagram, notice that the Vibration Team makes use of low-side N-channel MOSFETs to switch its payload, while the Pressure Team used high-side P-channel MOSFETs to provide switching. Switching on the high side made more sense for the Pressure Team, due to the large number of voltage rails needed for the operation of the circuit. The Vibration team decided it would be more convenient to use low-side N-channel MOSFETs on its switching circuitry, as it only needed one voltage rail for its electronics. This scheme works fine when both payloads are electrically isolated, but if both payloads ever were to come in contact with one another, current paths may form that would be potentially fatal for the electronics. And this is exactly what happened before final check-in.

When the payload is switched off via the activation line, the Vibration Team electronics are now at 14.8 V+ potential (including the ground plane), whereas the Pressure Team electronics remain at 0 voltage potential. When the incident occurred in which the two "ground planes" of the boards were connected via the metal bolts, the Vibration Team's ground plane, which was elevated to 14.8 volts, discharged into the 0 volt ground plane of the Pressure Team's electronics. In theory this should be okay under steady-state analysis of the current flow - the Vibration Team's electronics would find a path to ground through the ground plane of the Pressure Team's electronics, bypassing the Pressure Team's altogether. However, in the transient analysis of the current flow, there is actually a reverse-current path formed between the ground plane of the Pressure Team's electronics and the 7.4 volt rail, as shown below.

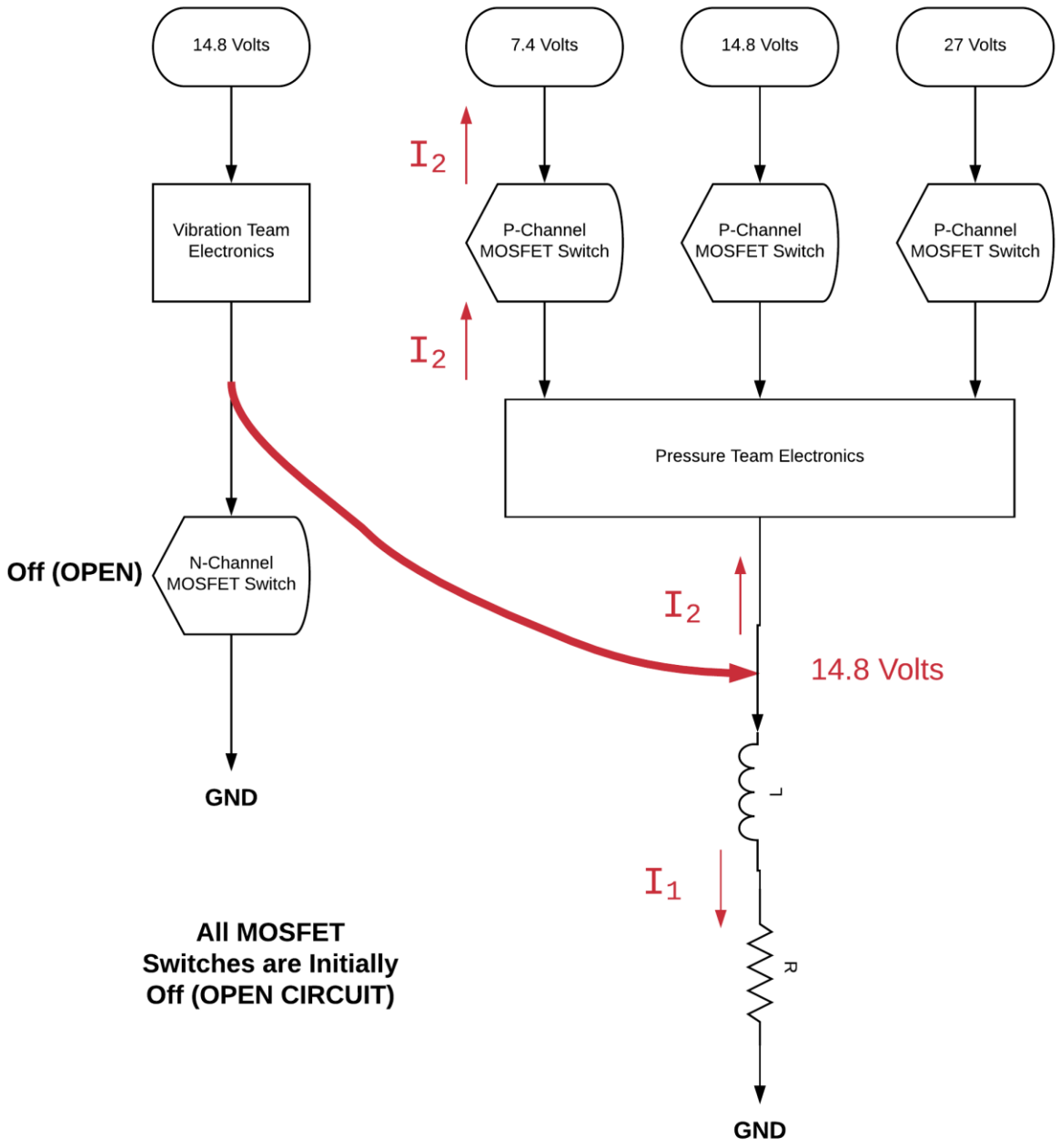

Figure 15: Transient Analysis of Integration Mishap

Figure 11 shows clearly what likely occurred when the two payloads were connected via their ground planes. The ground plane of the PCB, which appears like a short circuit to ground at low frequencies and DC, actually contains a great amount of inductance, which resists the change in voltage across it. When the bolt was initially connected to the payload, the ground plane of the Pressure Team's electronics briefly went to 14.8 Volts, which is higher than the 7.4

volt rail. Current could then easily flow through the 7.4 V P-channel MOSFET's intrinsic body diode up to the 7.4 volt rail. This rapid elevation of the 7.4 volt rail to close to 14.8 volts very likely killed a sensitive chip in the Beaglebone's electronics, rendering it non-functional, resulting in the failure of the Pressure Team's payload to collect any data whatsoever, as the Beaglebone failed to boot altogether.

7.0 Conclusions:

The payload design as a whole system appears to be complete and functional and continues to pass tests individually, albeit with a few flaws such as the inadequate sampling rate and the lower-than-expected analog gain. Despite these two inadequacies, the Pressure Team succeeded in building a functional data acquisition unit that, with some minor tweaking, could meet our success criteria. However, a severe problem occurred during payload integration when an unintended current path was established through the Vibration Isolation Team's board and the Pressure Team's board. This resulted in the Beaglebone Black becoming non-functional before launch, hence causing a failure to collect data. As of now, the team is confident that the DAQ would have collected data if this mishap did not occur. The team plans to verify this by performing an independent experiment as explained below in 8.0. In light of the absence of data, the system did survive the full testing and flight, thus demonstrating significant improvement over previous designs and a solution to the problems of previous years. This year's system has proven to be more modular and robust than the previous two iterations of this experiment.

8.0 Potential Follow-on Work:

The team has proposed to utilize Chris Cowan's rocketry experience and design a small scale project in order to test the system prior to any further large scale launches. Chris is a part of a high power rocketry club with the necessary certifications and such. As a result, the team will begin work on the design of a smaller rocket roughly 5-6" in diameter with a K450 rocket motor or similar. A smaller "canister" will be designed and fabricated to house the components similar to the system used for the sounding rocket. To produce data, the team plans to use a low cost, low-pressure sensor just to produce numbers rather than attempt any experimental use of data. This sensor is then wired to the conditioning board as the payload was originally designed, with the associated Beaglebone, PRUDAQ, signal conditioner board, and power supply. This payload eliminates the vibration isolation team's payload and strictly focuses on the capability and functionality of the pressure sensor team's electronics and software. After design, fabrication, testing and full integration the plan is to launch the rocket which will subject the system to very similar conditions. The results can then be analyzed to determine if data was written, if it was written fast enough, if the data is logical, etc. Overall, the goal is to produce a small scale mock scenario of RockSAT-C in the coming months to test the payload realistically and examine flaws to a greater extent.

9.0 Benefits to the Scientific Community:

Due to the absence of data, there is not a large benefit to the research of the advising professor, Professor Parziale. However, the team is now right on the edge of achieving the mission, with a much smaller obstacle than the previous years. Successful completion would then provide, if not the first, full flight data of this phenomenon, which can then be analyzed and studied further through further experiments and successive data collection.

10.0 Lessons Learned:

As the team continues to test the electronics, it appears more likely that the system was solid and successfully solved the previous years' problems. However, if this was the case, data would be present in this report. Thus, the most significant lesson learned through this was the communication across teams (aka between the pressure sensor and vibration team). If the integration was more carefully monitored by the pressure sensor team, we may have been able to catch the incident before it occurred. In addition, a large aspect of this problem was time management because the payload had to be integrated last minute. If integration was attempted prior between the teams, then this incident may have been noticed and could have been corrected by installing a new Beaglebone. Furthermore, this would allow for testing after integration to ensure the Digital Sampling Subsystem boots correctly and does indeed acquire data.

Another potential solution to make the electrical system more robust would be to add a polarity-protection diode to the power input. Such a diode would have entirely eliminated any reverse-current paths that occurred during the integration mishap, and would have been an extremely simple and easy addition to the electronics. In addition, if a polarity protection diode had been installed in the Vibration Isolation electronics, the incident which killed their first microcontroller board would not have happened. In essence, if polarity protection diodes had been implemented on this payload, both teams would likely have had collected data. A diode will be implemented on next year's payload.

Lastly, the experience of designing the Signal Conditioner PCB taught many lessons in the practical electronics. While one can learn about circuits in the classroom, there are many more things to consider when designing a circuit that will truly be built - especially circuits that will be turned into a PCB, where turnaround times are lengthy and there is great pressure to make sure the circuit works the first time. The design of the PCB was a process that took months, from designing the circuit, choosing components, and designing the PCB - all the way to building and testing it. Next year, if the team decides to design another PCB, it should consider two factors: the first is that PCB design is an iterative process. The design might not work the first time - but make sure that time is built into the schedule for multiple revisions in the event that the circuit doesn't work as expected. Secondly, soldering of the PCB is a very lengthy process, consuming a great deal of time and energy. Consider having the PCB manufactured

elsewhere by a pick and place service - this will save greatly on the time spent hunched over a soldering iron.

11.1 Appendices:

Hand Drawn Schematics of Signal Conditioner Board:

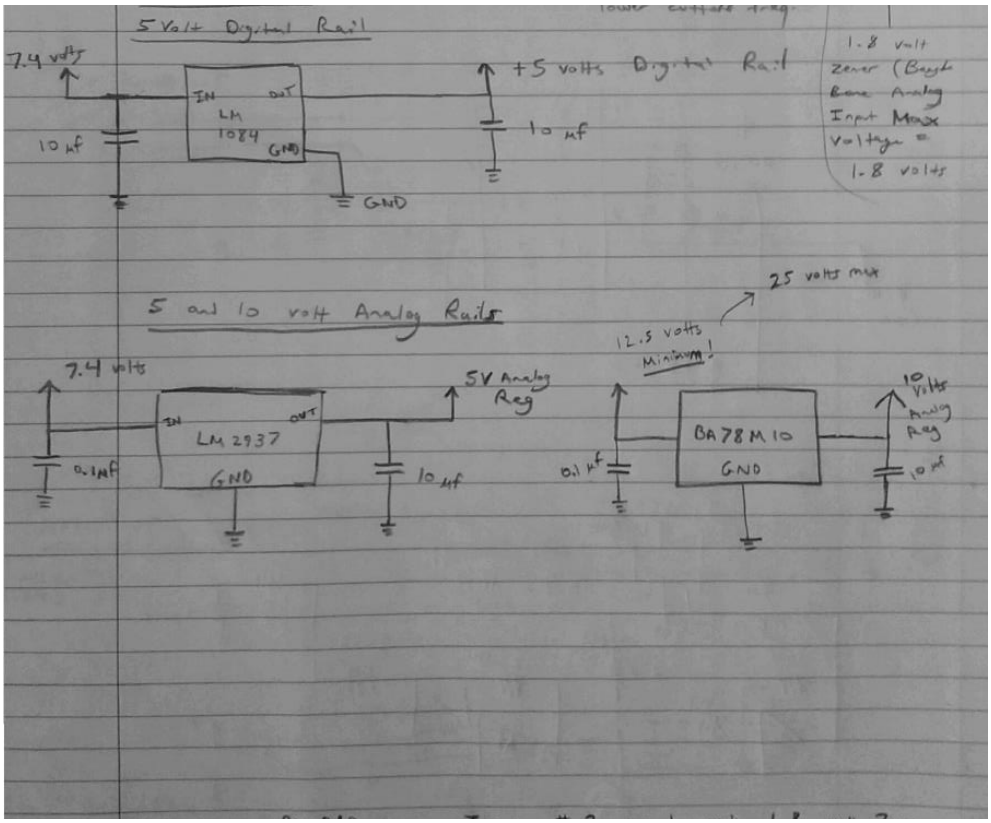

Figure 16: Analog Signal Conditioner Schematic, Power Supply

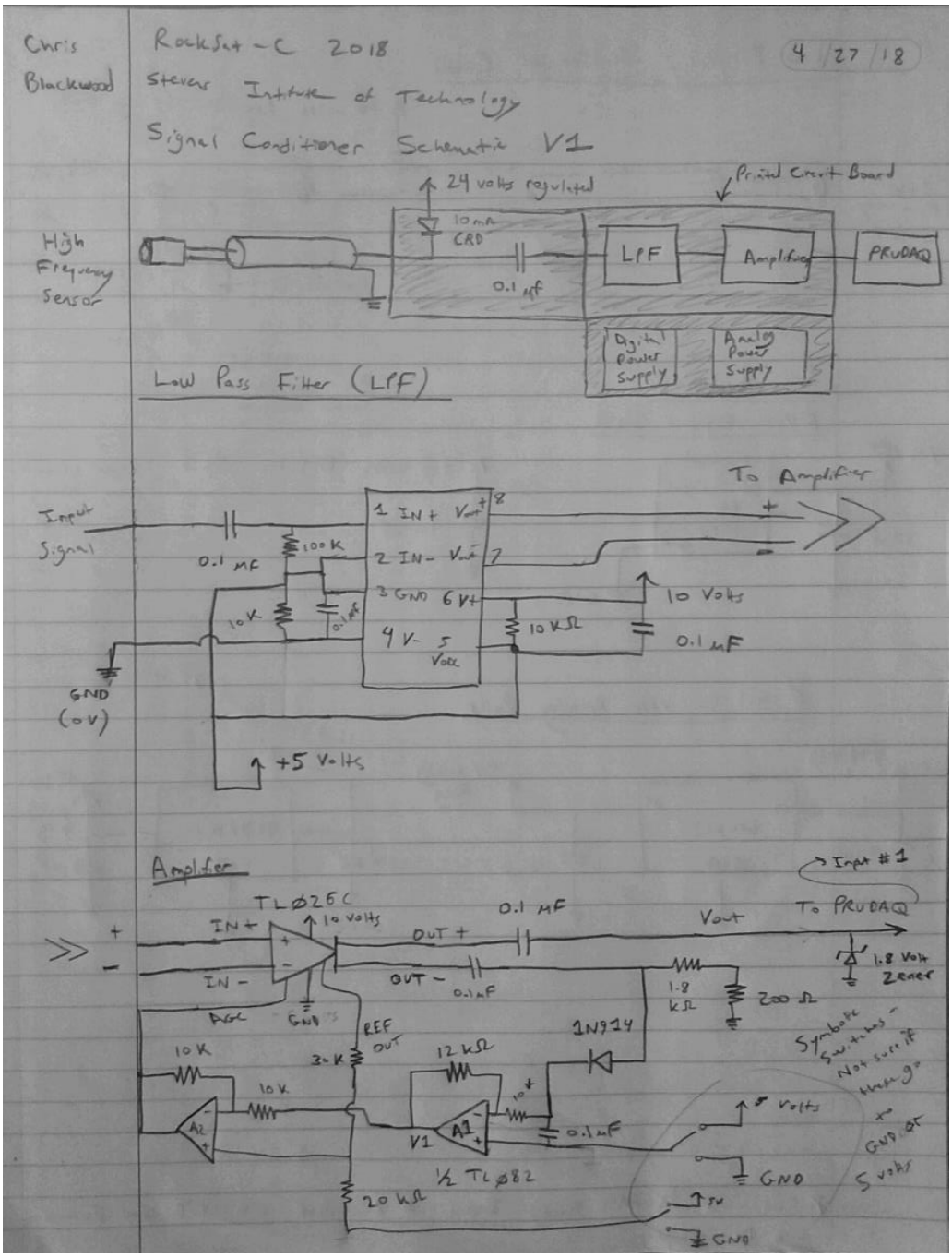

Figure 17: Analog Signal Conditioner Schematic

PCB Layout:

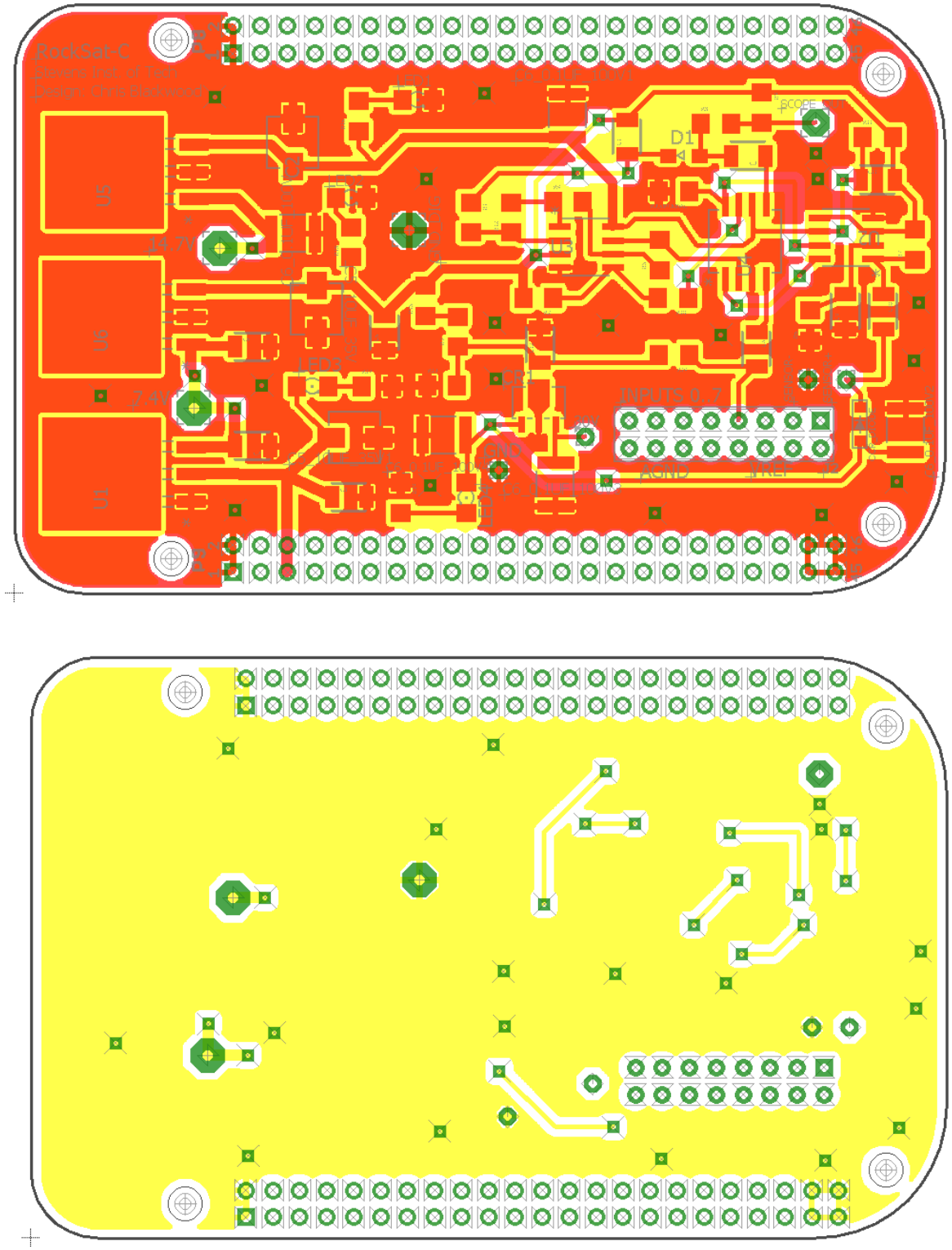

Figure 18 and 19: Signal Conditioner Board PCB Layout